SHORT TIME BEHAVIOUR OF DAM BREAK FLOW INVOLVING TWO LIQUIDS

A Thesis Submitted to
the Graduate School of Engineering and Sciences of
İzmir Institute of Technology
in Partial Fulfillment of the Requirements for the Degree of

DOCTOR OF PHILOSOPHY

in Mathematics

by
Damla ISIDICI DEMİREL

June 2018
İZMİR

We approve the thesis of **Damla ISIDICI DEMİREL**

Examining Committee Members:

———————————————————
Prof. Dr. Oğuz YILMAZ
Department of Mathematics, İzmir Institute of Technology

———————————————————
Prof. Dr. Oktay PASHAEV
Department of Mathematics, İzmir Institute of Technology

———————————————————
Assoc. Prof. Dr. Ünver ÖZKOL
Department of Mechanical Engineering, İzmir Institute of Technology

———————————————————
Prof. Dr. Halil ORUÇ
Department of Mathematics, Dokuz Eylül University

———————————————————
Assoc. Prof. Dr. Başak KARPUZ
Department of Mathematics, Dokuz Eylül University

29 June 2018

———————————————————
Prof. Dr. Oğuz YILMAZ
Supervisor, Department of Mathematics
İzmir Institute of Technology

———————————————————   ———————————————————
Prof. Dr. Engin BÜYÜKAŞIK   **Prof. Dr. Aysun SOFUOĞLU**
Head of the Department of   Dean of the Graduate School of
Mathematics   Engineering and Sciences

ACKNOWLEDGMENTS

ABSTRACT

SHORT TIME BEHAVIOUR OF DAM BREAK FLOW INVOLVING TWO LIQUIDS

The two dimensional dam break problem for wet bed case is investigated. The leading order and the second order problem are stated in nondimensional form. Solution to the leading order problem by using three different methods is given and explained in detail. Both Fourier series method and Galerkin method have difficulties on its own because of the singularity at the triple point. Although the singularity is ignored in Galerkin method, the method does not work except for the interface. Thus conformal mapping techniques is preferred because of the convenience and the strength of the complex analysis. The velocity profiles at whole boundary are obtained by using this conformal mapping. The second order solution of velocities are also obtained by using the same conformal mapping.

On the other hand, the domain decomposition method (DDM) is applied for the second order dam break problem of dry bed case. The leading order solution helped to determine the suitable parameters for DDM. The leading order and second order solution of the free surfaces give a more realistic shape using the Lagrangian solution at the upper corner point.

We assume this work contains useful and applicable methods in it for gravity driven flows and it will wake up different perspectives in readers mind.

ÖZET

İKİ SIVI İÇEREN BARAJ YIKILMASI AKIŞININ KISA ZAMAN DAVRANIŞI

İki boyutta ıslak zemin için baraj yıkılması problemi incelenmiştir. Birinci mertebeden ve ikinci mertebeden problem boyutsuz olarak ifade edilmiştir. Birinci mertebeden problemin çözümü üç farklı method kullanılarak verilmiş ve ayrıntılarıyla açıklanmıştır. Köşe noktadaki tekillik, Fourier serisi ve Galerkin yöntemlerinin her ikisinde de kendi içinde sıkıntılar meydana getirmiştir. Galerkin yönteminde tekillik ihmal edilmesine rağmen, yöntem arayüzey dışında işe yaramamıştır. Nitekim kompleks analiz tekniklerinin gücü ve uygunluğu nedeniyle, konformal dönüşüm tekniği tercih edilmiştir. Bu conformal mapping kullanılarak tüm sınırlarda hız profilleri elde edilmiştir. İkinci mertebeden hızların çözümleri de yine aynı conformal mapping kullanılarak elde edilmiştir.

Diğer taraftan, ikinci mertebeden kuru zemin için baraj yıkılması problemine alan ayrıştırma (domain decomposition, DDM) yöntemi uygulanmıştır. Birinci mertebe problemin çözümü DDM yöntemi için uygun parametreleri belirlemize yardım etmiştir. Birinci mertebeden ve ikinci mertebeden serbest su yüzeyi çözümleri, üst köşe noktadaki Lagrangian çözümü kullanılarak daha gerçeğe uygun bir şekil elde edilmiştir.

Bu çalışmanın, yerçekimi etkisi altındaki akışlar için kullanışlı ve uygulanabilir yöntemler içerdiğini ve okuyucunun aklında farklı bakış açıları uyandıracağını umuyoruz.

TABLE OF CONTENTS

LIST OF FIGURES

LIST OF TABLES

CHAPTER 1

INTRODUCTION

In this thesis, we examine the motion of two liquids interacting under the effect of gravity. The gravity driven flow starts when a vertical thin plate between the two flow regions abruptly removed. The sudden change in pressure leads to a singularity at velocities in the neighbourhood of the triple point (the upper point of the interface of the two liquids) and the bottom point (the lower point of the interface of the two liquids). The illustration in Fig. 1.1 makes these singularities understandable which are seen as jet-formation in real life. It is assumed in this thesis that the fluids are incompressible, inviscid and irrotational, and that initially fluids are at rest. For small times it is known that viscosity can be ignored Dressler (1952).
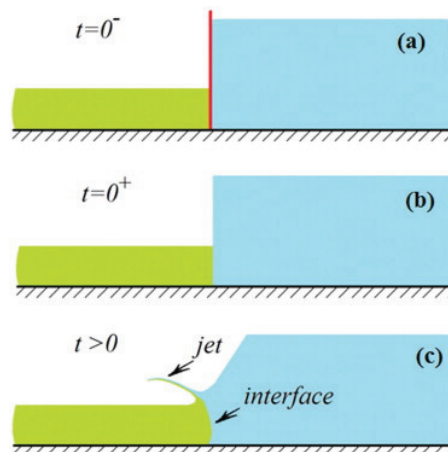
Figure 1.1. Scheme of the dam-break flow: (a) initially two liquids are at rest and separated with a vertical thin plate (dam); (b) the dam is removed at $t' = 0^+$ and flow starts; (c) Expected formation of a jet at the triple point

This idealized dam-break flow has a significant importance in civil engineering since the behaviour of jets at early stages provides foresight in developing the required design of a dam. A dam can be protected from the damages of natural or unnatural causes in emergency with the investigation of the early time evolution of the velocity profiles. Thus the motion of a fluid interacting with a solid body with a free surface

has a long history in fluid mechanics. The most interesting and important feature of this area is jet formations. "Mathematically, this results from the confluence of two analytical boundary conditions. Physically, this is not suprising, in view of the "splashing" which occurs when, for example, a falling body impacts with the free surface" Lin (1984). This makes the computation of the velocities and free surface displacements difficult near the point of intersection of the free surface and a moving body. The studies of gravity-driven flows due to dam breaking were started in 19. century by Ritter (1892) and confirmed by Pohle (1950) and Whitham (1892). Stoker extended the studies of Ritter to wet bed case J.J.Stoker (1958).

It is convenient to use potential theory to describe such jet-like formations when the initial stages of motion is considered. There are two approaches to describe the motion of a fluid and its related properties; Lagrangian description and Eulerian description. Studies by Pohle and Stoker used the Lagrangian description of motion. Pohle and Stoker stated that "The Lagrangian representation, has the far-reaching advantage that the independent space variables are the initial coordinates of the particles: the region occupied by the fluid is therefore a fixed region." But this is not suitable for the moving boundary problems since the exact location of liquid particles near the intersection points is unknown. This makes rather adequate to use Eulerian variables based on potential theory for the free-boundary problems. In the paper written by Pohle, Taylor expansion in time t' is applied to liquid displacement and the hydrodynamic pressure and the leading-order problem is analysed. Thus Pohle derived an early time solution close to the bottom point in Lagrangian variables which ignores the physical shape of the liquid free surface. Calculations in Eulerian variables also involve power series in time but represents the behaviour of the liquid free surface close to the bottom precisely. In both Lagrangian and Eulerian cases this solution will be the outer solution which needs to be corrected by an inner solution to provide a complete description of many extreme motion problems such as dam-break problem.

Another interesting wavemaker problem was carried out by Peregrine (1983) theoretically. This problem was a linearised model of the motion of a dam during an earthquake. Peregrine developed an outer solution by using a moving coordinate system which is fixed on the wavemaker. A similar analytical outer solution is obtained by Chwang (1983) by using a stationary coordinate system and identified the logarithmic singularity of the free surface at the intersection point. This paper emphasizes the nonlinear effect of the hydrodynamic pressure on an accelerating vertical plate. Both Chwang and Peregrine were aware of the necessity of the inner (local) solution valid near the corner point but

unable to determine it. The experimental contribution to this incomplete problem was achieved by Greenhow and Lin (1983). Greenhow took various photographs with different speeds and clarified the streamlines to provide inspiration for local solution. The singular behaviour of the leading order solution in time was also confirmed by Lin (1984) experimentally and numerically. Comparison of the experimental, numerical and analytical results is also given. Lin predicted that it is essential to study the problem in a small wavetank which makes the physical phenomena understandable. The numerical results help to describe the local behaviour of the free surface close to the intersection point. In the paper Lin (1984) used a new algorithm to overcome the numerical difficulties associated with the singularity by using sparse collocation point near the singularity anticipated grids. It is concluded that the pressure in the thin jet is very low and its contribution to the force can be ignored. But unfortunately, the analytical inner solution was still unknown. These studies are extended by Joo (1989) for general types of wavemaker velocities including capillary effects and for large time behaviour. However, such an analytical inner solution was successfully derived in a relevant problem concerning a uniformly accelerating wavemaker by King (1994) using matched asymptotic expansions and integral transform techniques. They obtained the thickness of the free surface as $O(-t^2 \log t)$ by equating the magnitude of the retained terms to the terms neglected in the dynamic boundary condition. This order of the magnitude of the jet thickness was the main motivation to construct an inner solution as discussed in Greenhow (1987). It was claimed that if the order of the magnitude of this jet thickness is a *priori*, the accuracy and efficiency of numerical calculation of such type of flows can be developed. This work is extended to an impulsively moved plate Needham et al. (2007) and finally an impulsively accelerating plate Needham et al. (2008). Recently, this work has generalized by considering the case of negative accelerations adding with the construction of the inner-inner asymptotic expansions by Gallagher (2015).

The singularity and the indicated mushroom-like jet behaviour were discovered by Stansby et al. (1998) for the wet-bed case of the dam-break problem. The theoretical analysis were consistent with the experimental results in a horizontal channel just after release. Long time structure is also conducted in this work experimentally and compared with the Stoker's shallow water solutions. Furthermore Korobkin and Yilmaz (2009), solved (dry-bed case) dam-break problem by using complex analytic function theory. But they needed the second order outer solution to derive the inner region dimension. In the master thesis of Isidici (2011), the methodology and findings from the paper King (1994) and applied to dam-break problem (dry-bed case) and the same solution as Korobkin

and Yilmaz was obtained. We noted a logarithmic singularity at the intersection point and explained the necessity of a local analysis and an inner solution. Subsequently the leading order dam-break problem of wet bed case is solved analytically and numerically by Yilmaz et al. (2013). However the inner region problem is not studied. They used the Fourier series method and compared the results by boundary element method with good agreement for sufficiently large γ, which is the ratio of densities. In this work, the types of the singularities at the triple point and at the bottom point are also identified as power singularity ($r^{-\alpha}$) and logarithmic singularity respectively.

1.1. Formulation

The unsteady problem of the motion of two inviscid immiscible fluids under the gravity at initial times is considered. At $t' = 0$ we have two stationary liquids at different levels seperated by a thin vertical plate at $x' = 0$, $0 < y' < H^+$ which represents a dam. The liquid in the right is described with density ρ^+ and lies in the region $x' > 0$, $0 < y' < H^+$ (Ω^+). Similarly the liquid in the left is described with density ρ^- and lies in the region $x' < 0$, $0 < y' < H^-$ (Ω^-) (see Fig. 1.2). H^+, H^- are the liquid depths and we assume $H^+ > H^-$ in our study since the shallower liquid is on the left. Dimensional variables are signified by primes.

The flow region is initially bounded by two horizontal free surfaces ($x' > 0$, $y' = H^+$ and $x' < 0$, $y' = H^-$) and the horizontal rigid impermeable bottom ($y' = 0$). The horizontal free-surface of the right liquid is denoted by $y' = \eta'^+(x', t')$ and the horizontal free-surface of the left liquid is denoted by $y' = \eta'^-(x', t')$. At time $t' = 0$, the dam instantaneously vanishes and the flow starts with a sudden change in the pressure distribution since the liquids are assumed to be incompressible. Just after the release there will be also initially vertical free-surface, its position is $x' = \xi'^+(y', t')$, $H^- < \xi'^+(y', t') < H^+$, and the interface, $x' = b'(y', t')$, and initially $0 < b'(y', t') < H^-$. Hence, we have three free-surfaces and an interface of the flow region $\Omega = \Omega^+ \cup \Omega^-$, which vary in time and have to be determined as a part of the solution. The free-surfaces $y' = \eta'^+$ and $y' = \eta'^-$ are functions of x' and t' since a liquid particle on them changes its position with time. For the same reason, $x' = \xi'^+$ and $x' = b'$ are functions of y' and t'. The pressure distributions in the liquids are hydrostatic initially; $p'^+(x', y', 0) = \rho^+ g(H^+ - y')$, $p'^-(x', y', 0) = \rho^- g(H^- - y')$ and the pressure on the free surfaces are atmospheric due to the Bernoulli's equation. The ratio of the constant densities ρ^+ and ρ^-, corresponding to the fluids in Ω^+ and Ω^-, is denoted by "$\gamma = \rho^-/\rho^+$" and g is the

gravitational acceleration.
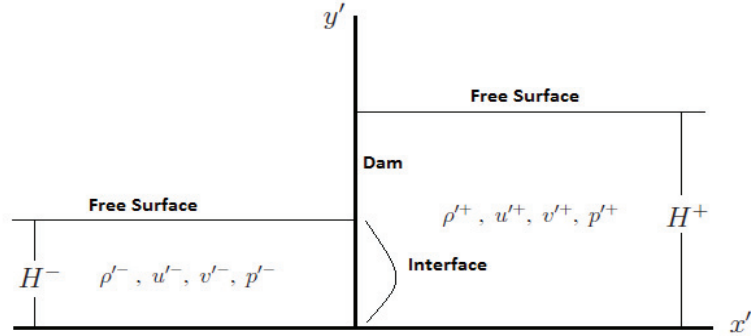
Figure 1.2. Flow region at the initial time instant $t' = 0$

Euler's equations of motion for incompressible flows are formed by the momentum equation

$$\rho \frac{D\mathbf{V}'}{Dt'} = \rho\vec{g} - \nabla'p' \tag{1.1}$$

and the incompressible form of the continuity equation

$$\nabla' \cdot \mathbf{V}' = 0 \tag{1.2}$$

in vector form, where the particle acceleration is

$$\frac{D\mathbf{V}'}{Dt'} = \frac{\partial\mathbf{V}'}{\partial t'} + (\mathbf{V}' \cdot \nabla)\mathbf{V}'$$

and $\nabla = (\partial/\partial x', \partial/\partial y')$ is the two-dimensional gradient operator in (x', y') cartesian coordinate system. Here $\mathbf{V}' = (u', v')$ is the velocity field. We denote the horizontal velocity by $u' = u'(x', y', t')$ and the vertical velocity $v' = v'(x', y', t')$. Hence, the two

dimensional problem (1.1)-(1.2) becomes

$$\frac{\partial u'^{\pm}}{\partial t'} + u'^{\pm}\frac{\partial u'^{\pm}}{\partial x'} + v'^{\pm}\frac{\partial u'^{\pm}}{\partial y'} = -\frac{1}{\rho^{\pm}}\frac{\partial p'^{\pm}}{\partial x'} \quad \text{in } \Omega^{\pm} \tag{1.3}$$

$$\frac{\partial v'^{\pm}}{\partial t'} + u'^{\pm}\frac{\partial v'^{\pm}}{\partial x'} + v'^{\pm}\frac{\partial v'^{\pm}}{\partial y'} = -\frac{1}{\rho^{\pm}}\frac{\partial p'^{\pm}}{\partial y'} - g \quad \text{in } \Omega^{\pm} \tag{1.4}$$

$$\frac{\partial u'^{\pm}}{\partial x'} + \frac{\partial v'^{\pm}}{\partial y'} = 0 \quad \text{in } \Omega^{\pm}. \tag{1.5}$$

in component form.

At $t' = 0$, since the liquid is at rest, the velocity components are zero, the free surfaces, the interface are at their initial positions $(t' = 0)$ and the pressure distribution is hydrostatic,

$$\left.\begin{array}{l} u'^{\pm}(x', y', 0) = v'^{\pm}(x', y', 0) = 0, \quad \eta'^{\pm}(x', 0) = H^{\pm} \\ \xi'^{+}(y', 0) = b'(y', 0) = 0 \quad \text{and} \quad p'^{\pm}(x', y', 0) = \rho^{\pm}g(H^{\pm} - y') \end{array}\right\} \quad \text{in } \Omega^{\pm}. \tag{1.6}$$

Furthermore we have six free-surface conditions (two for each surface). The dynamic conditions are expressed by the unsteady Bernoulli equation with the disappearance of the pressure on the free surfaces of the liquid. The kinematic conditions impose that fluid particles on the free surfaces of the liquid must stay on the free surfaces at any instant. Hence, we require

$$v'^{\pm} = \frac{\partial \eta'^{\pm}}{\partial t'} + u'^{\pm}\frac{\partial \eta'^{\pm}}{\partial x'} \quad \text{as a kinematic condition on } y' = \eta'^{\pm}(x', t'), \tag{1.7}$$

$$p'^{\pm}(x', \eta'^{\pm}, t') = 0 \quad \text{as a dynamic condition on } y' = \eta'^{\pm}(x', t') \tag{1.8}$$

and

$$u'^{+} = v'^{+}\frac{\partial \xi'^{+}}{\partial y'} + \frac{\partial \xi'^{+}}{\partial t'} \quad \text{as a kinematic condition on } x' = \xi'^{+}(y', t'), \tag{1.9}$$

$$p'^{+}(\xi'^{+}, y', t') = 0 \quad \text{as a dynamic condition on } x' = \xi'^{+}(y', t'). \tag{1.10}$$

6

Similarly, two interface conditions can be written as

$$u'^+ - v'^+ \frac{\partial b'}{\partial y'} = u'^- - v'^- \frac{\partial b'}{\partial y'} \quad \text{as a kinematic condition on } x' = b'(y', t'), \quad (1.11)$$

$$p'^+(b', y', t') = p'^-(b', y', t') \quad \text{as a dynamic condition on } x' = b'(y', t'). \quad (1.12)$$

Note that equations (1.11) and (1.12) imply the continuity of normal velocities to the interface and the continuity of pressure across the interface respectively. We also have a no-slip boundary condition at the rigid impermeable bottom;

$$v'^{\pm}(x', 0, t') = 0 \quad \text{on } y' = 0, \ x' \gtrless 0, \ t' > 0, \quad (1.13)$$

and the radiation conditions (the far-field conditions) in the two flow fields are,

$$u'^{\pm}, v'^{\pm} \to 0 \quad \text{as } x \to \pm\infty \quad (1.14)$$

consistent with the conditions: $\eta'^{\pm} \to H^{\pm}$ as $x \to \pm\infty$.

We need nondimensional equations to reformulate the equations for small times. Thus we introduce the following transformations to non-dimensionalize the equations (1.3) - (1.14),

$$x' = H^+ x, \qquad y' = H^+ y, \quad (1.15)$$

$$\eta'^{\pm} = H^+ \eta^{\pm}, \qquad \xi'^+ = H^+ \xi^+, \qquad b' = H^+ b, \quad (1.16)$$

$$t' = \sqrt{H^+/g}\, t, \qquad p'^{\pm} = p^{\pm} \rho^{\pm} g H^+. \quad (1.17)$$

Letting $\gamma = \dfrac{\rho^-}{\rho^+}$, $\delta = \dfrac{H^-}{H^+}$, we obtain a non-dimensional form of the boundary value problem, as shown in the next chapter. Note that $0 \le \delta \le 1$ implies that the shallower fluid is on the left.

In this thesis, we aim to find another way for the solution of the dam-break problem of wet-bed case as a contribution to the work presented in the paper Yilmaz et al. (2013) and investigate the second order problem.

With the methodologies, mentioned in the literature review, several flow problems can be solved. But in some problems using Fourier Series method, determining the coefficients of the Fourier series solutions of the leading order problem require inversion of a very large matrix. Therefore, there occurs a loss of accuracy depending on the computational tools since it leads to the solution of an infinite system of equations. While it is computationally expensive, it will also cause the convergency problems. This convergency problem is an expected problem since the Fourier series solution at the leading order is obtained without considering the singularity. But as an alternative method which does not require such an inversion is the variational method (also known as one-term Galerkin method) developed by Schwinger and Saxon (1968) in the study of waveguides concerning microwave radiation. Evans and Morris (1972), Dalrymple (1989) and Mandal and Dolai (1994) also used the same procedure for relevant problems and became successful in obtaining accurate results for the modulus of the reflection and transmission coefficients.

This variational method aims to provide methods for giving computationally effective results for quantities such as velocity, pressure and is studied in the thesis of Evans and Porter (1995) in detail and applied to several break water problems. He is motivated by the lack of an accurate and reliable method to cope with problems which involves sharp corners or edges on their geometries and extend the usual one-term Galerkin approtimation to N-term Galerkin approximation. The difficulty occurs with the presence of a singularity in the fluid velocity. At a sharp corner of a solid boundary, we can obtain the singularity by a simple analysis of the velocity field near the corner point. The method based on the construction of an integral equation form of the problem in terms of an unknown function related to the fluid velocity (or the pressure). Porter stated that "This is a direct consequence of the physical requirement that these two quantities be continuous everywhere in the fluid". Thus the substitution of an approximation function to the unknown function underlies the variational approach. Obviously we can say that the better the approximation gives the more the accurate results. He also point out that "the cruder approximations to the unknown functions in the integral equations give surprisingly good results too" as seen in Miles (1967). The advantage of the variational method is that the method only requires specifying the appropriate test functions which gives an accurate solution by a single calculation but the disadvantage is that the accuracy of the results depends on a better description of the unknown function. In this variational method, we first eliminate the singularity then find the series solution at the leading order in terms of the test functions. Therefore the convergency problem does not occur.

We can use conformal mapping techniques for fluid flow problems. To obtain the suitable conformal mapping requires precision but gives suprisingly good results for the solution of the leading order problem. The same method is used for the second order problem.

In this thesis, the second order outer problem of dam-break for dry-bed case ($H^- = 0$) is also studied to extend the content of the master study. Furthermore, the complete picture of the shape of the free surfaces with the second order solution is obtained using Lagrangian description for the upper part. Basically, the second order outer solution could be found by the Fourier series method just as is done with the first order solution. However the second order problem is far more complicated than the first order problem and it is convenient to use the domain decomposition method. The main idea of this method is to divide the whole fluid domain into suitable sub domains where solutions can be written as infinite series involving unknown coefficients, and then equate the truncated series at collocation points in the intersection of sub domains to derive the unknowns of the problem. The domain decomposition method is used successfully by Needham et al. (2008) to find the first outer solution in the problem of an inclined plate accelerating into a body fluid.

Domain decomposition methods suggest a convenient way to solve the complicated two and three dimensional nonlinear problems numerically by the concept of domain splitting instead of using arduous finite element approximations for the whole domain. As an example the numerical simulation of trasonic flow by the Schwarz-alternating method is solved by Glowinski et al. (1983) with the overlapped regions. They showed the efficiency and the stability of these methods by applying them to the several Poisson problems. Cai (2003) is also concentrated on one special group of these domain decomposition methods using overlapping subdomains and using the software diffpack. This study states that the convergence of the solution on the internal boundaries ensures the convergence of the solution in the entire solution domain. A detailed analysis of the domain decomposition methods, and of the "Schwarz method for overlapping domains" which is similar to the one adopted here, is given in Quarteroni and Valli (1999), where the mathematical foundations of the different approaches is provided.

We begin Chapter 2 by introducing the non-dimensional form of the boundary value problem. Taylor series expansions of the unknowns in time and resulting leading order problem is also stated in this chapter. We obtain the leading order solution and discuss the requirements for the convergency of the solution.

In Chapter 3, we apply Galerkin method to the boundary value problem using

suitable test functions at the interface. It gives fine results and validated by the analysis of the singularity at the triple point. But it is clearly stated that this variational method does not work for the boundary of the flow region.

In Chapter 4 and Chapter 5, the conformal mapping techniques are adapted to the leading order and the second order problem respectively. The derivation of the conformal mapping is expressed step by step in Chapter 3. The shape of the velocity profiles and the comparison of the velocity at the interface with the Galerkin solution are also included.

In Chapter 6, domain decomposition method is used to obtain the first and second order pressures. Furthermore the second order outer solution and the Lagrangian solution of the free surfaces are obtained.

CHAPTER 2

DAM BREAK PROBLEM (WET-BED CASE)

The initial stage of dam-break flow involving two liquids is solved both analytically and numerically in the paper Yilmaz et al. (2013). They used the Fourier Series Method (FSM) for the analytical solution and the Boundary Element Method (BEM) for the numerical solution of the problem given in unknown velocity potentials $\phi^{\pm}$. The graphs of the solutions for vertical and horizontal velocity is fitted well except for the case when the ratio of the densities (γ) is too large. In this chapter, we will study the same problem in unknown velocity, pressure, free-surface and interface variables in each region. The leading order problem will be constructed by using a short time expansions of the unknown variables to get a simplified initial form of the problem. Then we will obtain the FSM solution of the leading order pressures ($p_0^{\pm}$). The difficulty on evaluating the coefficients of the FSM solution and the necessity of another solution method is explained in detail in this chapter.

2.1. Mathematical Statement of the Problem
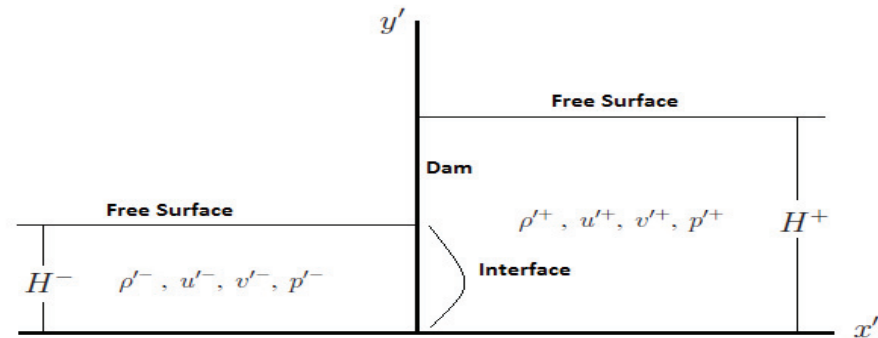
Figure 2.1. Flow region at the initial time instant $t' = 0$

A mathematical statement of the problem can now be written as a dimensionless

nonlinear boundary value problem in the form

$$u_x^+ + v_y^+ \;=\; 0 \quad \text{in } \Omega^+ , \tag{2.1}$$

$$u_t^+ + u^+ u_x^+ + v^+ u_y^+ \;=\; -p_x^+ \quad \text{in } \Omega^+ , \tag{2.2}$$

$$v_t^+ + u^+ v_x^+ + v^+ v_y^+ \;=\; -p_y^+ - 1 \quad \text{in } \Omega^+ , \tag{2.3}$$

$$v^+ = \eta_t^+ + u^+ \eta_x^+ , \quad p^+ \;=\; 0 \quad \text{on } y = \eta^+(x,t), \tag{2.4}$$

$$u^+ = \xi_t^+ + v^+ \xi_y^+ , \quad p^+ \;=\; 0 \quad \text{on } x = \xi^+(y,t), \tag{2.5}$$

$$v^+(x,0,t) \;=\; 0 \quad \text{on } y = 0, \tag{2.6}$$

$$\eta^+(x,0) = 1, \quad \xi^+(y,0) = b(y,0) = 0, \qquad u^+(x,y,0) = v^+(x,y,0) = 0, \tag{2.7}$$

$$\text{as } x \to \infty, \, u^+, v^+ \to 0 \text{ and } p^+ \to 1 - y, \tag{2.8}$$

$$u_x^- + v_y^- \;=\; 0 \quad \text{in } \Omega^- , \tag{2.9}$$

$$u_t^- + u^- u_x^- + v^- u_y^- \;=\; -p_x^- \quad \text{in } \Omega^- , \tag{2.10}$$

$$v_t^- + u^- v_x^- + v^- v_y^- \;=\; -p_y^- - 1 \quad \text{in } \Omega^- , \tag{2.11}$$

$$v^- = \eta_t^- + u^- \eta_x^- , \quad p^- \;=\; 0 \quad \text{on } y = \eta^-(x,t), \tag{2.12}$$

$$v^-(x,0,t) \;=\; 0 \quad \text{on } y = 0, \tag{2.13}$$

$$\eta^-(x,0) = \delta \quad \text{and} \quad u^-(x,y,0) \;=\; v^-(x,y,0) = 0, \tag{2.14}$$

$$\text{as } x \to \infty, \, u^-, v^- \to 0 \text{ and } p^- \to \delta - y, \tag{2.15}$$

$$u^+ - v^+ b_y = u^- - v^- b_y \quad \text{on } x = b(y,t) , \tag{2.16}$$

$$p^+(b,y,t) = \gamma p^-(b,y,t) \quad \text{on } x = b(y,t) . \tag{2.17}$$

The values $0 < \delta \le 1$ and $\gamma > 0$ are the two dimensionless parameters that characterise the problem.

2.2. Small-Time Behaviour ($t \to 0$)

A small-time solution to (6.1) - (2.17) may be developed by posing regular power series expansions in t:

$$u^{\pm} = u_0^{\pm}(x, y) + tu_1^{\pm}(x, y) + O(t^2), \quad v^{\pm} = v_0^{\pm}(x, y) + tv_1^{\pm}(x, y) + O(t^2),$$

$$\eta^{\pm} = \eta_0^{\pm}(x) + t\eta_1^{\pm}(x) + t^2\eta_2^{\pm}(x) + O(t^3), \quad \xi^+ = \xi_0^+(y) + t\xi_1^+(y) + t^2\xi_2^+(y) + O(t^3),$$

$$b = b_0(y) + tb_1(y) + t^2b_2(y) + O(t^3), \quad p^{\pm} = p_0^{\pm}(x, y) + tp_1^{\pm}(x, y) + O(t^2).$$

as $t \to 0$ with $\mathbf{x} = O(1)$.

Since $u^{\pm}(x, y, 0) = 0$ and $v^{\pm}(x, y, 0) = 0$, we conclude that $u_0^{\pm} = 0$ and $v_0^{\pm} = 0$. Similarly since $\eta^+(x, 0) = 1$, $\eta^-(x, 0) = \delta$, $\xi^+(y, 0) = 0$ and $b(y, 0) = 0$, we conclude that $\eta_0^+ = 1$, $\eta_0^- = \delta$, $\xi_0^+ = 0$ and $b_0 = 0$. Now the small-time solution expansions to (6.1) - (6.5) can be written as

$$u^{\pm} = tu_1^{\pm}(x, y) + O(t^2), \qquad v^{\pm} = tv_1^{\pm}(x, y) + O(t^2),$$

$$\eta^+ = 1 + t\eta_1^+(x) + t^2\eta_2^+(x) + O(t^3), \qquad \eta^- = \delta + t\eta_1^-(x) + t^2\eta_2^-(x) + O(t^3),$$

$$\xi^+ = t\xi_1^+(y) + t^2\xi_2^+(y) + O(t^3), \qquad b = tb_1(y) + t^2b_2(y) + O(t^3),$$

$$p^{\pm} = p_0^{\pm}(x, y) + tp_1^{\pm}(x, y) + O(t^2)$$

We substitute the above expansions into the equations (6.1) - (6.5). We have the following boundary value problems at the leading order,

$$\left. \begin{array}{c} u_{1,x}^+ + v_{1,y}^+ = 0 \quad \text{in } \Omega^+, \\ u_1^+ = -p_{0,x}^+ \quad , \qquad v_1^+ = -p_{0,y}^+ - 1 \quad \text{in } \Omega^+, \\ v_1^+(x, 0) = 0, \quad \eta_2^+ = \frac{1}{2}v_1^+(x, 1), \quad \xi_2^+ = \frac{1}{2}u_1^+(0, y), \\ p_0^+(x, 1) = 0, \quad p_0^+(0, y) = 0 \end{array} \right\} \qquad (2.18)$$

with $u_1^+, v_1^+ \to 0$ and $p_0^+ \to 1 - y$ as $x \to \infty$.

$$\left. \begin{array}{c} u_{1,x}^- + v_{1,y}^- = 0 \quad \text{in } \Omega^-, \\ u_1^- = -p_{0,x}^- \quad , \qquad v_1^- = -p_{0,y}^- - 1 \quad \text{in } \Omega^-, \\ v_1^-(x, 0) = 0, \quad \eta_2^- = \frac{1}{2}v_1^-(x, \delta), \\ p_0^-(x, \delta) = 0 \end{array} \right\} \qquad (2.19)$$

with $u_1^-, v_1^- \to 0$ and $p_0^- \to \delta - y$ as $x \to -\infty$.

13

Then the problem (2.18) and (2.19) are equivalent to the boundary value problems

$$\left.\begin{array}{l} \Delta p_0^+ = 0 \quad \text{in } \Omega^+, \\ p_{0,y}^+(x,0) = -1, \quad p_0^+(x,1) = 0 \end{array}\right\} \tag{2.20}$$

with $p_0^+ \to 1 - y$ as $x \to \infty$,

$$\left.\begin{array}{l} \Delta p_0^- = 0 \quad \text{in } \Omega^-, \\ p_{0,y}^-(x,0) = -1, \quad p_0^-(x,\delta) = 0 \end{array}\right\} \tag{2.21}$$

with $p_0^- \to \delta - y$ as $x \to -\infty$, and

$$P_0^+(0,y) = \left\{ \begin{array}{ll} \gamma P_0^-(0,y), & 0 < y < \delta \\ 0, & \delta < y < 1 \end{array} \right. \tag{2.22}$$

$$P_{0,x}^+(0,y) = P_{0,x}^-(0,y), \quad 0 < y < \delta. \tag{2.23}$$

2.3. Fourier Series Solutions, Leading Order

Solutions to the problems (2.20) and (2.21) may be found by the separation of variables method in the form of the following series of solutions of Laplace's equation which already satisfy the bed boundary condition.

$$p_0^+(x,y) = 1 - y + \sum_{n=0}^{\infty} C_n \cos\left((2n+1)\frac{\pi}{2}y\right) e^{-(2n+1)\frac{\pi}{2}x}, \tag{2.24}$$

$$p_0^-(x,y) = \delta - y + \sum_{n=0}^{\infty} D_n \cos\left((2n+1)\frac{\pi}{2\delta}y\right) e^{(2n+1)\frac{\pi}{2\delta}x}. \tag{2.25}$$

The coefficients C_n and D_n can be determined by using the leading order free-surface condition and the leading order interface conditions (2.22)-(2.23), as a solution of an infinite system of equations. Trying to solve this system directly using the orthogonality
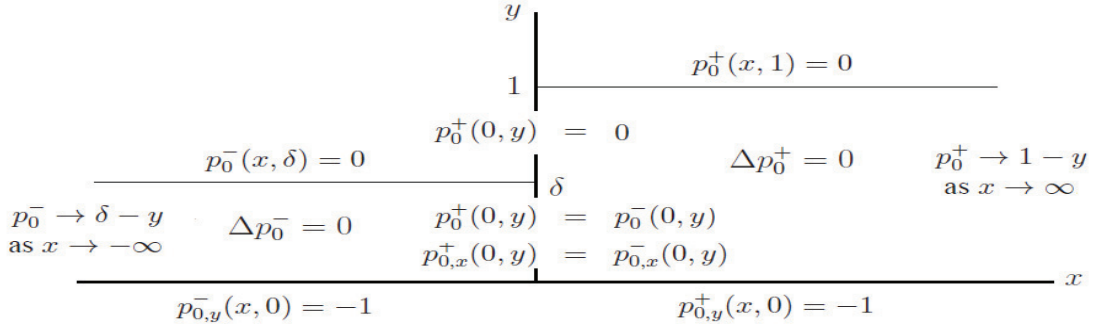
Figure 2.2. Dimensionless flow region at the initial time instant $t = 0$

property of cosine terms in (2.24) and (2.25) and the conditions (2.22)-(2.23) give

$$D_m = \sum_{n=0}^{N} \alpha_{nm} \lambda_n C_n, \qquad\qquad m = 0, 1, \ldots, M \quad (2.26)$$

$$C_m = \frac{4\gamma \sin^2\left(\frac{\lambda_m \delta}{2}\right) - 2}{\lambda_m^2} - \sum_{n=0}^{M} \gamma \alpha_{mn} \lambda_n D_n, \qquad m = 0, 1, \ldots, N \quad (2.27)$$

where N, M are the numbers in (2.26) and (2.27) we truncate the infinite sum in the series solution of $p_0^+(x, y)$ and $p_0^-(x, y)$ respectively and

$$\lambda_n = \frac{(2n + 1)\pi}{2} \quad \text{and} \quad \alpha_{nm} = \frac{2\delta(-1)^m \cos(\delta \lambda_n)}{\delta^2 \lambda_n^2 - \lambda_m^2}.$$

The system (2.26)-(2.27) leads to the following $(N + 1) \times (N + 1)$ square system

$$\sum_{k=0}^{N} \left[\delta_{km} + \sum_{n=0}^{M} \gamma \alpha_{mn} \alpha_{kn} \lambda_n \lambda_k \right] C_k = \frac{4\gamma \sin^2\left(\frac{\lambda_m \delta}{2}\right) - 2}{\lambda_m^2}, \qquad m = 0, 1, \ldots, N \quad (2.28)$$

where δ_{km} is the *Kronecker delta*. Solution to the unknown coefficients $C_0, C_1, \ldots, C_N$ can be obtained by solving (2.28). Then substituting C_n's into (2.26) gives $D_0, D_1, \ldots, D_M$.

15

Table 2.1. Relative error (RE) on pressure condition due to singularity at the triple point for $\delta = 1/2$

RE_N	RE_{300}	RE_{301}	RE_{302}	RE_{303}
	0.367	0.440	0.163	0.275

But we have loss of convergency notwithstanding the large N, M and hence nearly big relative errors (Table 2.1) due to singularity at the triple point $(0, \delta)$ with this direct calculation.

Therefore we need another method which is computationally efficient and gives accurate results even for small number of terms. This method is *Galerkin's variational method*.

CHAPTER 3

VARIATIONAL APPROXIMATION, LEADING ORDER

The variational method is a reliable method when we have a lack of the accuracy on somewhere on the geometry of fluid flow. This method is easy to apply and gives computationally effective results. But there is only one key point for this method which needs care. That is, it is hard to choose suitable test functions for the approximation of the unknown function. In this chapter, we first describe the method and then apply it to the dam break problem. The choice of the test function for the horizontal velocity on the interface is explained in detail. At the end of this chapter, we will see that the variational method works well for the horizontal velocity on the interface but it is not appropriate for the vertical free surface.

3.1. Method

The eigenfunction expansion approach constitutes a starting point for this method. The basic principles of the method are behind the application of eigenfunction expansions to the solution of problems in fluid flow. The fluid domain is divided into two (or more) regions and in each of the regions we have an appropriate eigenfunction solution form of the unknown variable which is constructed to satisfy all the boundary conditions of the problem except on the interface of the subregions. The interface conditions are the continuity of fluid velocity and pressure. Substitution of the eigenfunction solutions in each region to the interface condition (matching eigenfunction expansions) leads to a singular integral equation for the unknown function related to physical quantities. An approximation to the unknown function can be found using orthogonal expansions involving trigonometric functions which leads to a large system of equations with a large number of unknown coefficients. McIver (1985) used such type of approximation for the general problem of two arbitrarily spaced surface piercing barriers in finite depth but the convergence of the approximated solution was slow and the accuracy was undetermined. An alternative approximation method is used by Dalrymple (1989) to estimate the value of reflection coefficient for a problem of abrupt channel transitions of water waves. He used the variational method which is developed by Schwinger and Saxon (1968) and known

as the Schwinger variational method. The variational approach (equal to the Galerkin method in this thesis) is simple and a favoured way for approximating required quantities and is computationally inexpensive.

The most powerful application of this approach is outlined in the PhD thesis of Porter (1995). He examined the method in detail and adapted the method to several water wave scattering problems. The success of the method depends on a plausible choice of the test functions to reflect the physical behaviour of the unknown variable. The singular integral equation generated by the matching conditions on the interface for a function $u(y)$ related to the unknown velocity in the flow region across the interface (denoted by L_g) can be written in its simplest form as,

$$\mathcal{K}u = \psi_0, \quad y \in L_g, \tag{3.1}$$

where ψ_0 will be defined later and the operator $\mathcal{K}$ is positive-definite and self-adjoint. We need a quantity $(u, \psi_0)_{L_g} = A$ to clarify the availability of the method. The inner product is defined as

$$(u, v)_{L_g} = \int_{L_g} u(y)\overline{v(y)}dy. \tag{3.2}$$

Let us define the functional $J : L_2(L_g) \to \mathbf{R}$ by

$$J(\tilde{u}) = (\psi_0, \tilde{u}) + (\tilde{u}, \psi_0) - (\mathcal{K}\tilde{u}, \tilde{u}), \text{for any } \tilde{u} \in L_2(L_g), \tag{3.3}$$

where $L_2(L_g)$ is the L_2 space on the interval L_g. Then

$$
\begin{aligned}
J(\tilde{u}) &= J(u + (\tilde{u} - u)) \\
&= J(u) + (\psi_0 - \mathcal{K}u, \tilde{u} - u) + (\tilde{u} - u, \psi_0 - \mathcal{K}u) - (\mathcal{K}(\tilde{u} - u), \tilde{u} - u) \\
&= J(u) - (\mathcal{K}(\tilde{u} - u), \tilde{u} - u) \\
&\leq J(u)
\end{aligned}
$$

since $\mathcal{K}u = \psi_0$ and $\mathcal{K}$ is positive. From the definition of J by (3.3), $J(u) = (u, \psi_0) = A$,

so we can write

$$J(\tilde{u}) \leq A. \tag{3.4}$$

Equality holds if and only if $\tilde{u} = u$ and $J(\tilde{u})$ has a stationary value A at $\tilde{u} = u$ where A is real and positive. Notice also that,

$$J(u) - J(\tilde{u}) = (\mathcal{K}(\tilde{u} - u), \tilde{u} - u) = O(\|\tilde{u} - u\|^2). \tag{3.5}$$

which means if $\tilde{u}$ is a first order approximation to u, the approximation to A will be second order accurate. Galerkin's method involves approximating u as a series of test functions such as

$$\tilde{u}(y) = \sum_{n=0}^{N} a_n u_n(y), \tag{3.6}$$

where $u_n(y)$ are the test functions and a_n's are the unknown coefficients. The approximation (3.6) satisfies in the components of the subspace spanned by the approximation. The stationary value of $J(u)$ is obtained when its spatial derivatives with respect to each coefficient is zero,

$$\frac{\partial J(\tilde{u})}{\partial a_n} = 0, \quad n = 0, \ldots, N. \tag{3.7}$$

Thus we get $N + 1$ equations for $N + 1$ unkowns. This system can be solved to get a_n, and hence gives the approximation. But an alternative and easier procedure to obtain the coefficients a_n is, instead of satisfying $\mathcal{K}u - \psi_0 = 0$ exactly, to impose

$$(\mathcal{K}\tilde{u} - \psi_0, u_m) = 0, \quad m = 0, \ldots, N, \tag{3.8}$$

or

$$\sum_{n=0}^{N} a_n (\mathcal{K}u_n, u_m) = (\psi_0, u_m), \quad m = 0, \ldots, N, \tag{3.9}$$

19

which can be written in the matrix form

$$
\begin{pmatrix}
(\mathcal{K}u_0, u_0) & (\mathcal{K}u_0, u_1) & \cdots & (\mathcal{K}u_0, u_N) \\
\vdots & & & \vdots \\
(\mathcal{K}u_N, u_0) & (\mathcal{K}u_N, u_1) & \cdots & (\mathcal{K}u_N, u_N)
\end{pmatrix}
\begin{pmatrix}
a_0 \\
\vdots \\
a_N
\end{pmatrix}
=
\begin{pmatrix}
(\psi_0, u_0) \\
\vdots \\
(\psi_0, u_N)
\end{pmatrix}. \quad (3.10)
$$

By writing $K_{mn} = (\mathcal{K}u_n, u_m)$ and $F_{m0} = (\psi_0, u_m)$, and introducing the matrix notation $\mathbf{K} = \{K_{mn}\}$, $\mathbf{F} = (F_{00}, \ldots, F_{n0})^T$ we may eliminate the coefficients a_n. Whilst not going into detail, it should be mentioned that there are a number of issues that we must consider in the choice of test functions: the set of function $\{u_0(y), \ldots, u_N(y)\}$ should be complete in $L_2(L_g)$ so that convergence is assured as $N \to \infty$ and the elements of $\mathbf{K}$, $\mathbf{F}$ should be easy to compute.

3.2. Application of Galerkin Method to Dam Break Problem

We start with applying the Galerkin method and assume that we have the same fluids in right and left regions, *i.e.*, $\gamma = 1$. Assume that $P_{0,x}^+(0, y) = F(y)$, $0 < y < 1$, a priori unknown function, then using the kinematic interface condition (2.23) and the series solution of $P_0^+(x, y)$ (2.24) we have,

$$
P_{0,x}^+(0, y) = \sum_{n=0}^{\infty} C_n(-\lambda_n) \cos(\lambda_n y) = F(y), \quad 0 < y < 1.
$$

Multiplying the above equation by $\cos(\lambda_m y)$ and integrating over $(0, 1)$ gives

$$
C_n = -\frac{2}{\lambda_n} \int_0^1 F(y) \cos(\lambda_n y) dy, \quad n = 0, 1, 2, \ldots \quad (3.11)
$$

On the other hand using the kinematic interface condition (2.23) and the series solution of $P_0^-(x, y)$ (2.25) we have,

$$
P_{0,x}^-(0, y) = \sum_{n=0}^{\infty} D_n(\frac{\lambda_n}{\delta}) \cos(\frac{\lambda_n}{\delta} y) = F(y), \quad 0 < y < \delta.
$$

20

Multiplying the last equation by $\cos(\frac{\lambda_m y}{\delta})$ and integrating over $(0, \delta)$ gives

$$D_n = \frac{2}{\lambda_n} \int_0^{\delta} F(y) \cos(\frac{\lambda_n y}{\delta}) dy, \quad n = 0, 1, 2, \ldots \tag{3.12}$$

Now let us substitute (3.11), (3.12) into the series solution of $P_0^+(x,y)$ (2.24), $P_0^-(x,y)$ (2.25) respectively and use (2.22) to get the integral equation form of the problem,

$$1 - y - \int_0^1 F(\xi) K(y, \xi) d\xi = \begin{cases} \delta - y + \int_0^{\delta} F(\xi) K(\frac{y}{\delta}, \frac{\xi}{\delta}) d\xi, & 0 < y < \delta \\ \\ 0 & , \quad \delta < y < 1, \end{cases} \tag{3.13}$$

where

$$K(y, \xi) = \sum_{n=0}^{\infty} \frac{2}{\lambda_n} \cos(\lambda_n \xi) \cos(\lambda_n y) \tag{3.14}$$

is a symmetric kernel. The equation (3.13) can also be written as

$$1 - y = \begin{cases} \delta - y + \int_0^1 F(\xi) K(y, \xi) d\xi + \int_0^{\delta} F(\xi) K(\frac{y}{\delta}, \frac{\xi}{\delta}) d\xi, & 0 < y < \delta \\ \\ \int_0^1 F(\xi) K(y, \xi) d\xi & , \quad \delta < y < 1. \end{cases} \tag{3.15}$$

Now, make an approximation

$$F(y) \simeq \tilde{F}(y) = \sum_{n=0}^{L} a_n f_n(y), \quad y \in (0, 1), \tag{3.16}$$

where we have yet to define the test functions $f_n(y)$ and the a_n's are the unknown constants. Substituting this approximation (3.16) into (3.15), multiplying through by $f_m(y)$

and integrating over $(0, 1)$,

$$\int_0^1 (1 - y) f_m(y) dy \tag{3.17}$$

$$= \int_0^1 f_m(y) \left\{ \begin{array}{ll} \delta - y + \int_0^1 \left(\sum_{n=0}^L a_n f_n(\xi) \right) K(y, \xi) d\xi \\ + \int_0^\delta \left(\sum_{n=0}^L a_n f_n(\xi) \right) K(\frac{y}{\delta}, \frac{\xi}{\delta}) d\xi, & 0 < y < \delta, \\ \int_0^1 \left(\sum_{n=0}^L a_n f_n(\xi) \right) K(y, \xi) d\xi, & \delta < y < 1 \end{array} \right\} dy,$$

where $m = 0, 1, \ldots, L$. After substituting the kernels (3.14) in (3.17), we get,

$$\int_0^1 (1 - y) f_m(y) dy \tag{3.18}$$

$$= \int_0^1 f_m(y) \left\{ \begin{array}{ll} \delta - y + \int_0^1 \sum_{n=0}^L a_n f_n(\xi) \sum_{r=0}^\infty \frac{2}{\lambda_r} \cos(\lambda_r \xi) \cos(\lambda_r y) \, d\xi \\ + \int_0^\delta \sum_{n=0}^L a_n f_n(\xi) \sum_{r=0}^\infty \frac{2}{\lambda_r} \cos(\frac{\lambda_r \xi}{\delta}) \cos(\frac{\lambda_r y}{\delta}) \, d\xi, & 0 < y < \delta, \\ \int_0^1 \sum_{n=0}^L a_n f_n(\xi) \sum_{r=0}^\infty \frac{2}{\lambda_r} \cos(\lambda_r \xi) \cos(\lambda_r y) \, d\xi, & \delta < y < 1 \end{array} \right\} dy,$$

for $m = 0, 1, \ldots, L$. We interchange the integrals with the summations and the integral terms in (3.18) are organized with respect to their variables and intervals, and thus

$$\int_0^1 (1 - y) f_m(y) dy = \int_0^\delta (\delta - y) f_m(y) dy \tag{3.19}$$

$$+ \sum_{n=0}^L a_n \left[\sum_{r=0}^\infty \frac{2}{\lambda_r} \int_0^1 \cos(\lambda_r \xi) f_n(\xi) d\xi \int_0^\delta \cos(\lambda_r y) f_m(y) dy \right]$$

$$+ \sum_{n=0}^L a_n \left[\sum_{r=0}^\infty \frac{2}{\lambda_r} \int_0^\delta \cos(\frac{\lambda_r \xi}{\delta}) f_n(\xi) d\xi \int_0^\delta \cos(\frac{\lambda_r y}{\delta}) f_m(y) dy \right]$$

$$+ \sum_{n=0}^L a_n \left[\sum_{r=0}^\infty \frac{2}{\lambda_r} \int_0^1 \cos(\lambda_r \xi) f_n(\xi) d\xi \int_\delta^1 \cos(\lambda_r y) f_m(y) dy \right]$$

where $m = 0, 1, \ldots, L$. Then, we write the terms in (3.19) as a single sum over n,

$$\int_0^1 (1-y)f_m(y)dy = \int_0^\delta (\delta-y)f_m(y)dy \tag{3.20}$$

$$+ \sum_{n=0}^L a_n \left[\sum_{r=0}^\infty \frac{2}{\lambda_r} \int_0^\delta \cos(\frac{\lambda_r\xi}{\delta})f_n(\xi)d\xi \int_0^\delta \cos(\frac{\lambda_r y}{\delta})f_m(y)dy \right.$$

$$+ \sum_{r=0}^\infty \frac{2}{\lambda_r} \int_0^1 \cos(\lambda_r\xi)f_n(\xi)d\xi \int_0^\delta \cos(\lambda_r y)f_m(y)dy$$

$$+ \left. \sum_{r=0}^\infty \frac{2}{\lambda_r} \int_0^1 \cos(\lambda_r\xi)f_n(\xi)d\xi \int_\delta^1 \cos(\lambda_r y)f_m(y)dy \right]$$

where $m = 0, 1, \ldots, L$. We combine the same integrals terms in (3.20) with consecutive intervals,

$$\int_0^1 (1-y)f_m(y)dy = \int_0^\delta (\delta-y)f_m(y)dy \tag{3.21}$$

$$+ \sum_{n=0}^L a_n \left[\sum_{r=0}^\infty \frac{2}{\lambda_r} \int_0^\delta \cos(\frac{\lambda_r\xi}{\delta})f_n(\xi)d\xi \int_0^\delta \cos(\frac{\lambda_r y}{\delta})f_m(y)dy \right.$$

$$+ \left. \sum_{r=0}^\infty \frac{2}{\lambda_r} \int_0^1 \cos(\lambda_r\xi)f_n(\xi)d\xi \int_0^1 \cos(\lambda_r y)f_m(y)dy \right]$$

where $m = 0, 1, \ldots, L$. Letting,

$$\int_0^1 \cos(\lambda_r\xi)f_n(\xi)d\xi = I_{rn}^{(1)}, \quad \int_0^1 \cos(\lambda_r\xi)f_m(\xi)d\xi = I_{rm}^{(1)}, \tag{3.22}$$

$$\int_0^\delta \cos(\frac{\lambda_r\xi}{\delta})f_n(\xi)d\xi = I_{rn}^{(\delta)}, \quad \int_0^\delta \cos(\frac{\lambda_r\xi}{\delta})f_m(\xi)d\xi = I_{rm}^{(\delta)} \quad \text{and} \tag{3.23}$$

$$\int_0^1 (1-y)f_m(y)dy = J_m^{(1)}, \quad \int_0^\delta (\delta-y)f_m(y)dy = J_m^{(\delta)} \tag{3.24}$$

(3.21) becomes,

$$J_m^{(1)} = J_m^{(\delta)} + \sum_{n=0}^L a_n \left[\sum_{r=0}^\infty \frac{2}{\lambda_r} \left(I_{rn}^{(\delta)} I_{rm}^{(\delta)} + I_{rn}^{(1)} I_{rm}^{(1)} \right) \right], \tag{3.25}$$

where $m = 0, 1, \ldots, L$. Evaluation of the integral terms in (3.25) gives the following

23

general system,

$$F_m = \sum_{n=0}^{L} a_n K_{mn}, \quad m = 0, \ldots, L, \tag{3.26}$$

where

$$K_{mn} = \sum_{r=0}^{\infty} \frac{2}{\lambda_r} \left(I_{rn}^{(\delta)} I_{rm}^{(\delta)} + I_{rn}^{(1)} I_{rm}^{(1)} \right) \tag{3.27}$$

is a symmetric matrix and,

$$F_m = J_m^{(1)} - J_m^{(\delta)}. \tag{3.28}$$

Next, we will choose $f_m(y)$ depending on the type of the singularity. So a singularity analysis of the triple point $(0, \delta)$ is required.

3.2.1. Analysis of The Singularity at the Triple Point, $(0, \delta)$

An analysis of the flow close to the corner point $(0, \delta)$ can be done by solving the local problem in unknown velocity potential shown in Fig. 3.1. The coordinates (x', y') are the shifted coordinates where $x' = x$ and $y' = y - \delta$. The solution of the horizontal
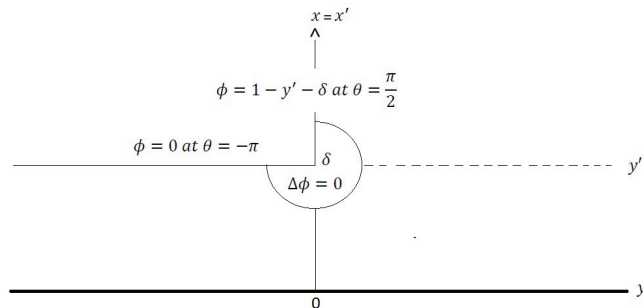
Figure 3.1. Local problem around the corner point

velocity near the corner point can be obtained by using the relation $u = \phi_{x'}$ as

$$u(y') = \frac{2}{3}c\sin\left(\frac{1}{3}(2\pi - \theta)\right)(y - \delta)^{-1/3} - \frac{2}{3\pi}(1 - \delta)\sin(\theta)(y - \delta)^{-1}, \qquad (3.29)$$

which reveals that $u(y) \sim (y - \delta)^{-1/3}$ asymptotically, as $y \to \delta^-$ and c is an arbitrary constant. By using the behaviour of $u(y)$ as $y \to \delta^-$ and since $\phi_y = 0$ on $y = 0$, $u(y)$ can be continued as an even function of y across $y = 0$ by the reflection principle (Fig. 3.2). This continuation gives us the behaviour $u(y) \sim (-\delta - y)^{-1/3}$ as $y \to -\delta^+$. Thus we must multiply the function $u(y)$ with $\{(\delta - y)(\delta + y)\}^{1/3} = \{\delta^2 - y^2\}^{1/3}$ to get rid of the singularity as $y \to \delta^-$. Therefore the even continuous function $\{\delta^2 - y^2\}^{1/3}u(y)$ can be expanded in $(0, 1)$ in a complete set of even Jacobi polynomials (hypergeometric polynomials, see Appendix E),

$$f_m(y) = |\delta^2 - y^2|^{-1/3}P_{2m}^{(-\frac{1}{3}, -\frac{1}{3})}(y), \qquad (3.30)$$

where P_{2m} is the $2m^{th}$ order Jacobi polynomial for $\alpha = \beta = -\frac{1}{3}$.
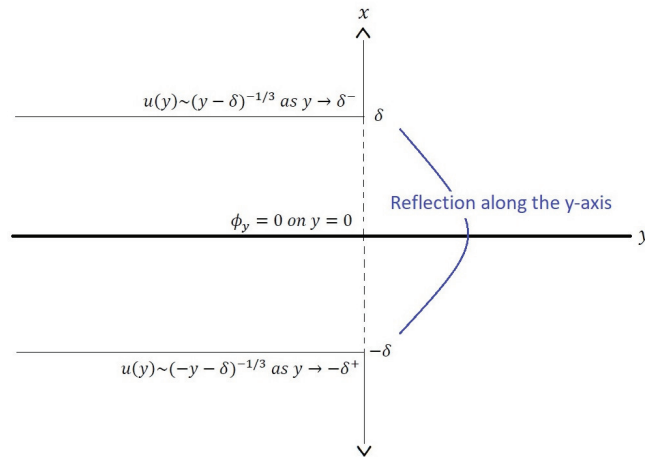
Figure 3.2. Reflection principle for the horizontal velocity on the interface

3.3. Numerical Procedures and Results

To solve (3.26) we must first compute K_{mn}, F_m given by (3.27) and (3.28) for $m, n = 0, \ldots, L$. Each entry in K_{mn} consists of an infinite sum which is evaluated by truncation. In order to choose the truncation point, we will analyse the order of the terms in (3.27) with respect to r. For the integral $I_{rn}^{(\delta)}$ in (3.27), after putting $\xi = \delta t$ in (3.23), we get ($Erdélyi$, 1954)

$$I_{rn}^{(\delta)} = \frac{\delta^{1/3}(-1)^n \sqrt{\pi}\, \Gamma(2n - \frac{4}{3}) J_{2n+\frac{1}{6}}(\lambda_r)}{2^{5/6}(2n)!(\lambda_r)^{1/6}}$$

where Γ is the Gamma function and J_n is the Bessel function of first kind of order n. Using the asymptotic behaviour of $J_n(x)$ for large x (Abromowitz&Stegun,1965) it is readily shown that, as $r \to \infty$,

$$I_{rn}^{(\delta)} I_{rm}^{(\delta)} = O\left(\frac{1}{r^{4/3}}\right).$$

For the integral $I_{rn}^{(1)}$ in (3.27), we use integration by parts which is a particularly easy procedure for developing asymptotic approximations to many kinds of integrals. After one integration by parts, we see that

$$I_{rn}^{(1)} \sim \frac{(-1)^r P_{2n}^{(-\frac{1}{3}, -\frac{1}{3})}(\frac{1}{\delta})}{|\delta^2 - 1|^{1/3}\lambda_r} \quad \text{as } r \to \infty.$$

Hence,

$$I_{rn}^{(1)} I_{rm}^{(1)} = O\left(\frac{1}{r^2}\right).$$

Thus the infinite series (3.27) decays like $O(1/r^3)$ and we truncate the sum at $R = 40$ in our numerical computations where the relative error is minimized.

On the other hand, it is computationally too expensive to evaluate the integrals inside the matrices $\mathbf{K} = \{K_{mn}\}$ and $\mathbf{F} = (F_0, \ldots, F_m)^T$ in (3.26) in closed form. Therefore we need a higher order numerical integration method which gives highly accurate

results and works much faster than direct calculation. Thus we use 'Roomberg Integration' method to resolve this difficulty. Thus we get the matrices $\mathbf{K}$ and $\mathbf{F}$ in (3.26) where

$$\mathbf{K}\,\mathbf{a} = \mathbf{F}. \tag{3.31}$$

But the matrix $\mathbf{K}$ has a large condition number, for instance $\kappa(\mathbf{K}) = 2.862 \times 10^{51}$ for the parameters $\gamma = 1$, $\delta = 1/2$, $M = N = 40$, $L = 6$ and $\delta = 1/2$, which means the matrix $\mathbf{K}$ is numerically very close to a singular matrix (nearly singular). So standard methods such as LU decomposition fail due to accumulation of round of errors. Further there exists a powerful technique to deal with sets of equations or matrices that are either singular or else numerically very close to singular known as '*Singular Value Decomposition*', or SVD. With SVD, the $M \times M$ matrix $\mathbf{K}$ can be written as the product of an $M \times N$ column-orthogonal matrix $\mathbf{U}$, a $M \times N$ diagonal matrix $\mathbf{W}$ with positive or zero elements (the singular values), and the transpose of an $M \times M$ orthogonal matrix $\mathbf{V}$. Hence the system (3.31) becomes

$$\mathbf{U}\,\mathbf{W}\,\mathbf{V^T}\,\mathbf{a} = \mathbf{F},$$

and the solution is

$$\mathbf{a} = \mathbf{V}\,\mathbf{W}^{-1}\,\mathbf{U^T}\,\mathbf{F}.$$

This is much more computational work than direct method of solution, but it has impeccable numerical properties. Instead of calculating the inverse of a singular matrix, we just calculate $\mathbf{V}$, $\mathbf{W}$ and $\mathbf{U}$. Hence we get the solution of (3.26), *i.e.* $\mathbf{a}$, and the approximation $\tilde{F}(y)$ (3.16) for $\gamma = 1$, $\delta = 1/2$, $M = N = 40$ and $L = 6$ are given with the comparison of the series solution in Fig. 3.3 and Fig. 3.4. We see that the Galerkin's method works fine.

In Fig. (3.5), horizontal velocity at the interface is shown, which is exactly the same as the result in Yilmaz et al. (2013).

On the other hand, we use same test functions for the part at the top of the interface. But when we compare the solutions with Yilmaz et al. (2013), we see in Fig. 3.6 that there is a seperation in Fig. 3.6.

Figure 3.3. Comparison of the horizontal velocity of the interface with Galerkin's method ($M = N = 40$ and $L = 6$) and series solution (with $N = 100$)

Table 3.1. Substitution of the Galerkin's solution into (3.26)

y	0.05	0.1	0.2	0.3	0.4	0.45
left	0.5760	0.5243	0.4183	0.3074	0.1826	0.1076
right	0.5770	0.5257	0.4191	0.3051	0.1817	0.1117
y	0.5	0.55	0.6	0.7	0.8	0.9
left	0.0006	0.0123	0.0029	-0.0054	0.0022	-0.0010
right	0	0	0	0	0	0

To see the error, we substitute our solution into (3.13) and get the following Table 3.1.

Thus we need to try to solve the system (3.26) by using another computational tool to find the cause of the error.

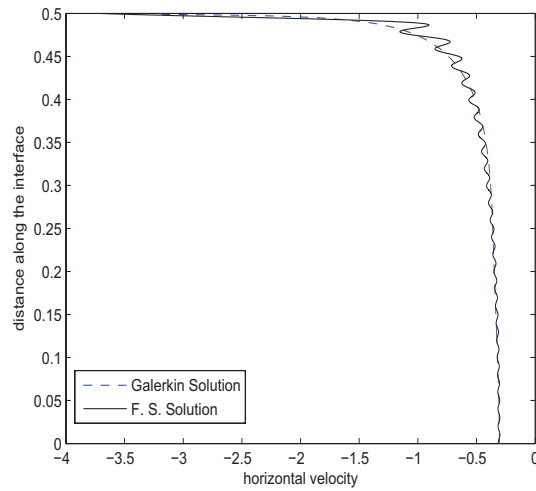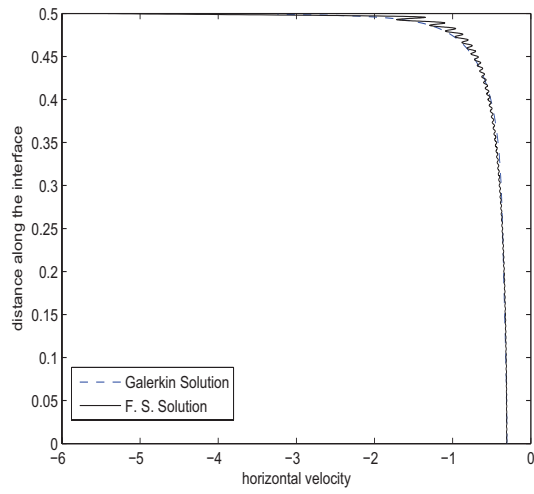Figure 3.4. Comparison of the horizontal velocity of the interface with Galerkin's method ($M = N = 40$ and $L = 6$) and series solution (with $N = 300$)
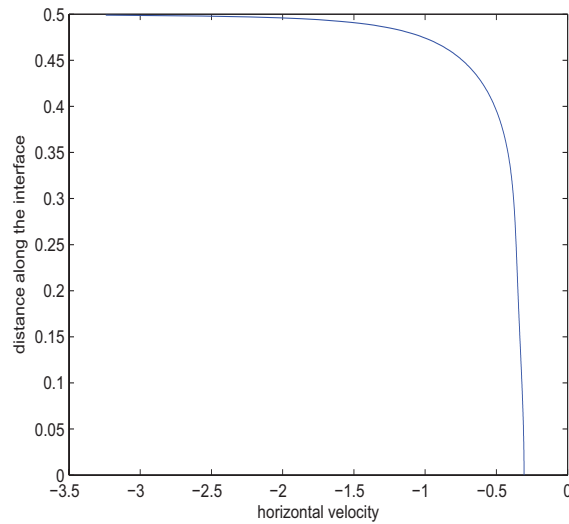

Figure 3.5. Horizontal velocity of the interface for $\gamma = 1$, $\delta = 1/2$, $M = N = 40$ and $L = 6$
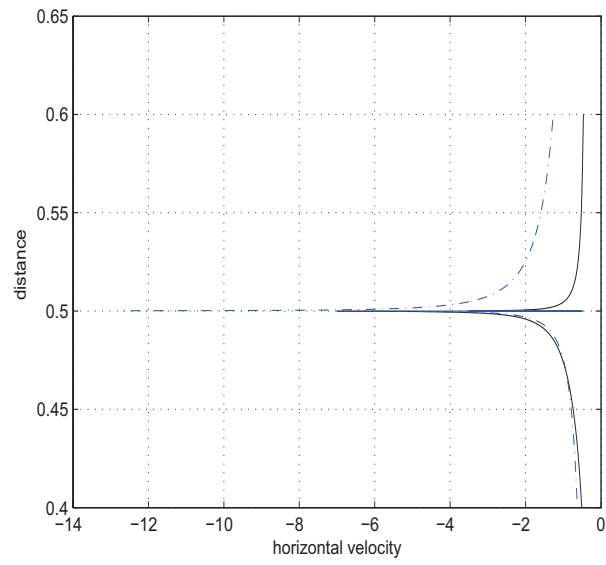
Figure 3.6. Comparison of the horizontal velocity around the corner point (dashed-dotted lines represents Yilmaz, Korobkin & Iafrati (2013) solution)

CHAPTER 4

SOLUTION BY CONFORMAL MAPPING, LEADING ORDER

We employ complex analysis to supply harmonic functions for the solution to the two-dimensional Laplace equation. So the conformal mapping of the analytical functions allows for complicated problems in fluid flow to be solved with simpler geometry. Thus we take the advantage of the compatibility of conformal mapping for the analytical solution of the dam-break problem. In this chapter, conformal mapping techniques are used and a suitable conformal mapping which maps the fluid region to the lower half plane is obtained. We find the form of the mapping and hence to find the leading order velocity profiles at the lower half plane. The shape of the leading order velocity profiles are plotted on the whole boundary of the flow region. The image of the interface is also calculated with the support of some numerical tools. In addition to the solutions, the asymptotic analysis of the velocities are investigated near the corner point which indicates the order of the singularity precisely. Finally, we end this chapter with the comparison of the horizontal velocity profiles by using conformal mapping solution and Galerkin solution at the interface.

4.1. Leading Order Pressure for the Same Fluid on Either Side of the Dam

For the leading order problem; we know that in the case of equal densities $\rho^+ = \rho^-$ ($\gamma = 1$), leading order pressures and normal derivatives of the leading order pressures are equal at the interface. Therefore we can ignore the interface and consider the leading order problem in one unknown pressure in the fluid region with different behaviours at $\pm$ infinity. So, our aim is to find the solution of this problem. Thus by using this solution and analysing the singularity, we aim to decide which test functions for the variational methods are suitable for the corresponding regions. By recalling the problem, which was derived in Chapter 2 (Fig. 2.2), we sketch Fig. 4.1 representing the same problem for equal densities on each side.
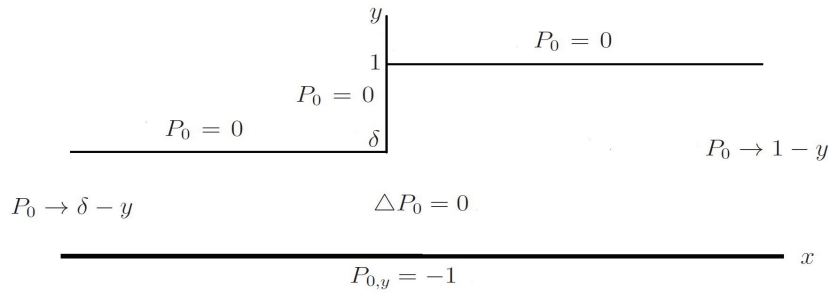
Figure 4.1. Flow region at the initial time instant $t = 0$ for equal densities in each side

To solve this problem, we first use the transformation $Q = P_0 + y - 1$. Then the problem Fig. 4.1 becomes Fig. 4.2 with the unknown variable Q, Notice that problem
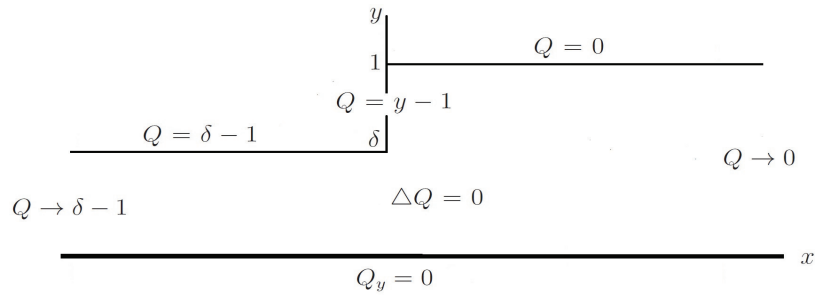
Figure 4.2. Flow region at the initial instant $t = 0$ with the boundary condition for Q

for Q, Fig. 4.2 is simpler than the problem for P_0 since the condition at $+\infty$ becomes homogeneous. Now we can apply the conformal mapping to this problem.

4.1.1. Mapping of the Fluid Domain Onto a Lower Half Plane

We choose to transform the fluid region onto the lower half plane with a suitable conformal mapping. Let $z = Z(\zeta)$ be the conformal mapping which maps the lower half
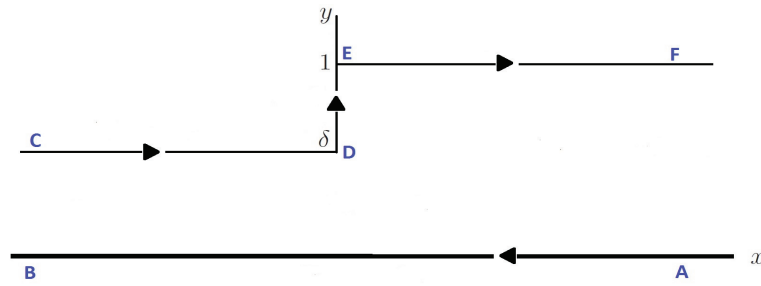
Figure 4.3. The boundary of the fluid domain described clockwise, using letters to label significant points

plane $(\eta < 0)$ Fig. 4.3 onto the fluid region with the specified direction Fig. 4.4. The point k which will be determined later in ζ-plane corresponds to point 1 in z-plane. Since
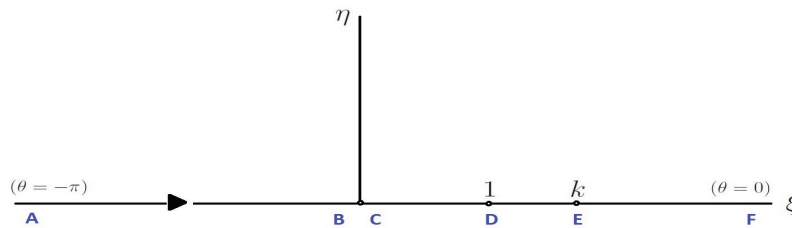
Figure 4.4. The lower half plane. The letters correspond to letters in Fig. 4.3 and describe the domain boundary clockwise

y is bounded as $x \to \infty$, we can write

$$Z(\zeta) \sim A_1 \ln \zeta + A_0 \quad (\zeta \to \infty)$$

where A_1 is a real, A_0 is a complex constant and $\zeta = re^{i\theta}$, $-\pi < \theta < 0$ in $\eta < 0$. We see that $\ln |\zeta| \to \infty$ and $\arg \zeta$ is bounded as $\zeta \to \infty$ in the lower-half plane which is the same with $x \to \infty$ and y is bounded as $z \to \infty$ in the flow domain. Using the behaviour

33

of $Z(\zeta)$ as $\zeta \to \infty$ *i.e.* at the points A ($\theta = -\pi$) and F ($\theta = 0$), we have $A_1 = 1/\pi$ and $\Im(A_0) = 1$. Hence,

$$Z(\zeta) \sim \frac{1}{\pi} \ln \zeta + i + \Re(A_0) \quad (\zeta \to \infty). \tag{4.1}$$

On the other hand, we can write

$$Z(\zeta) \sim B_1 \ln \zeta + B_0 \quad (\zeta \to 0)$$

where B_1 is a real, B_0 is a complex constant and $\zeta = re^{i\theta}$, $-\pi < \theta < 0$ in $\eta < 0$. We see that $\ln |\zeta| \to -\infty$ and $Arg(\zeta)$ is bounded as $\zeta \to 0$ in the lower-half plane which is the same with $x \to -\infty$ and y is bounded as $z \to -\infty$ in the flow domain. Using the behaviour of $Z(\zeta)$ as $\zeta \to 0$ *i.e.* at the points B ($\theta = -\pi$) and C ($\theta = 0$), we have $B_1 = \delta/\pi$ and $\Im(B_0) = \delta$. Hence,

$$Z(\zeta) \sim \frac{\delta}{\pi} \ln \zeta + i\delta + \Re(B_0) \quad (\zeta \to 0). \tag{4.2}$$

Let's consider the function

$$\tilde{Z}(\zeta) = \ln \left[\frac{dZ}{d\zeta} \zeta \pi \right]$$

which is analytic in $\eta < 0$ and on the boundary $\zeta = \xi - i0$

$$\frac{dZ}{d\zeta} \zeta \pi = \frac{dx}{d\xi} \xi \pi > 0 \quad (\Im[\tilde{Z}(\xi - i0)] = 0) \quad \text{on } AB, CD, EF$$

$$\frac{dZ}{d\zeta} \zeta \pi = i \frac{dy}{d\xi} \xi \pi > 0 \quad (\Im[\tilde{Z}(\xi - i0)] = \frac{\pi}{2}) \quad \text{on } DE$$

i.e. $\Im[\tilde{Z}(\xi - i0)] = \pi/2$, where $1 < \xi < k$, and zero on the rest of the boundary and $\tilde{Z}(\zeta) \to 0$ as $\zeta \to \infty$ (see (4.1)). Therefore $-i\tilde{Z}$ is also analytic in $\eta < 0$ and $\Re[\tilde{Z}(\xi - i0)(-i)] = \pi/2$, where $1 < \xi < k$, and zero on the rest of the boundary and $-i\tilde{Z}(\zeta) \to 0$ as $\zeta \to \infty$. Hence the solution of this BVP-AF can be written as (see

Appendix B)

$$-i\tilde{Z}(\zeta) = \frac{i}{\pi} \int_1^k \frac{\pi}{2} \frac{d\tau}{\tau - \zeta}.$$

Evaluation of the integral gives,

$$\tilde{Z}(\zeta) = -\frac{1}{2} \ln \left(\frac{k - \zeta}{1 - \zeta} \right) = \ln \left[\frac{dZ}{d\zeta} \zeta \pi \right].$$

Then the derivative of the mapping is obtained as

$$\frac{dZ(\zeta)}{d\zeta} = \frac{1}{\pi \zeta} \left(\frac{\zeta - 1}{\zeta - k} \right)^{1/2}. \qquad (4.3)$$

We define local polar coordinates (r, α) and (ρ, β) for the points 1 and k in ζ plane:

$$\xi = 1 + re^{i\alpha} \quad (-\pi < \alpha < 0) \qquad (4.4)$$
$$\xi = k + \rho e^{i\beta} \quad (-\pi < \beta < 0) \qquad (4.5)$$

the square roots in (4.3) are understood as shown in Fig. 4.5
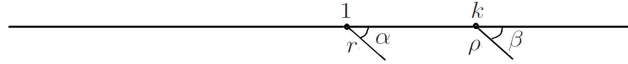
Figure 4.5. The description of the square roots centered at 1 and k

$$\left(\frac{\xi - 1}{\xi - k} \right)^{1/2} = \left(\frac{r}{\rho} \right) e^{i \frac{\alpha - \beta}{2}}.$$

Hence,

$$\frac{dZ}{d\xi} = \frac{1}{\pi\xi}\left(\frac{1-\xi}{k-\xi}\right)^{1/2}, \quad \text{on } AB, \tag{4.6}$$

$$\frac{dZ}{d\xi} = \frac{1}{\pi\xi}\left(\frac{1-\xi}{k-\xi}\right)^{1/2}, \quad \text{on } CD, \tag{4.7}$$

$$\frac{dZ}{d\xi} = i\frac{1}{\pi\xi}\left(\frac{\xi-1}{k-\xi}\right)^{1/2}, \quad \text{on } DE, \tag{4.8}$$

$$\frac{dZ}{d\xi} = \frac{1}{\pi\xi}\left(\frac{\xi-1}{\xi-k}\right)^{1/2}, \quad \text{on } EF. \tag{4.9}$$

Hence on the boundary of the flow region, the conformal mapping $z = Z(\zeta)$ is calculated as,

$$z = x + iy = \frac{1}{\pi}\int_k^\xi \frac{1}{\tau}\sqrt{\frac{\tau-1}{\tau-k}}d\tau + i \quad \text{on } EF,$$

$$z = x + iy = \frac{i}{\pi}\int_1^\xi \frac{1}{\tau}\sqrt{\frac{\tau-1}{k-\tau}}d\tau + i\delta \quad \text{on } DE,$$

$$z = x + iy = -\frac{1}{\pi}\int_\xi^1 \frac{1}{\tau}\sqrt{\frac{1-\tau}{k-\tau}}d\tau + i\delta \quad \text{on } CD.$$

To find the point k, consider this mapping on the DE part of the boundary

$$i\frac{dy}{d\xi} = \frac{i}{\pi\xi}\left(\frac{\xi-1}{k-\xi}\right)^{1/2}, \tag{4.10}$$

taking integral of both sides with respect to ξ from 1 to k and multiplying both sides by π gives

$$\pi(1-\delta) = \int_1^k \frac{1}{\xi}\left(\frac{\xi-1}{k-\xi}\right)^{1/2} d\xi,$$

$$= \int_1^k \frac{\xi-1}{\xi}\frac{d\xi}{\sqrt{(\xi-1)(k-\xi)}}.$$

Using the change of variables $\xi = \frac{k-1}{2}\cos\alpha + \frac{k+1}{2}$ and then trigonometric substitu-

tion, we obtain

$$\pi(1 - \delta) = \pi(1 - \frac{1}{\sqrt{k}})$$

which gives $k = 1/\delta^2$.

To evaluate the values of x on AB are not easy as we did for the other parts of the boundary. Consider the mapping (4.3)

$$\frac{dx}{d\xi} = \frac{1}{\pi\xi}\left(\frac{1-\xi}{k-\xi}\right)^{1/2} \quad \text{on } AB$$

or equivalently

$$\frac{d\xi}{dx} = \pi\xi\left(\frac{k-\xi}{1-\xi}\right)^{1/2} \quad \text{on } AB. \tag{4.11}$$

The first order nonlinear ODE (4.11) can be solved numerically with an initial condition $\xi = \xi_0$ at $x = 0$. Then we obtain ξ values for $\xi < \xi_0$ on AB in the ζ-plane, corresponding to x values for $x > 0$ on AB in the z-plane. We can also obtain ξ values for $\xi_0 < \xi < 0$ on AB in the ζ-plane and corresponding to x values for $x < 0$ on AB in the z-plane by solving the same ODE (4.11) in negative direction.

To find the value of ξ_0, consider the values of x as an integral by using (4.6) on AB such that

$$x = \frac{1}{\pi}\int_{\xi_0}^{\xi}\frac{1}{\tau}\sqrt{\frac{1-\tau}{k-\tau}}d\tau \quad \text{for } \xi_0 < \xi < 0$$

which is equivalent to

$$x = \frac{1}{\pi}\int_{\xi_0}^{\xi}\frac{1}{\tau}\left(\frac{1}{\sqrt{k}} + \left[\sqrt{\frac{1-\tau}{k-\tau}} - \frac{1}{\sqrt{k}}\right]\right)d\tau \quad \text{for } \xi_0 < \xi < 0. \tag{4.12}$$

Then consider the integral (4.12) as $\xi \to 0^-$ *i.e.* consider the values of x on AB as

$\xi \to 0^-$, we have

$$x \sim \frac{\delta}{\pi} \ln|\xi| - \frac{\delta}{\pi} \ln|\xi_0| + \frac{\delta(1-k)}{\pi} \int_{\xi_0}^{0} \frac{d\tau}{\sqrt{k-\tau}(\sqrt{k-k\tau} + \sqrt{k-\tau})}$$

and using equation (4.2), we can write

$$\Re(B_0) = -\frac{\delta}{\pi} \ln|\xi_0| + \frac{\delta(1-k)}{\pi} \int_{\xi_0}^{0} \frac{d\tau}{\sqrt{k-\tau}(\sqrt{k-k\tau} + \sqrt{k-\tau})}. \qquad (4.13)$$

On the other hand, the values of x on CD as an integral by using (4.7) on CD are

$$x = -\frac{1}{\pi} \int_{\xi}^{1} \frac{1}{\tau} \sqrt{\frac{1-\tau}{k-\tau}} d\tau \quad \text{for } 0 < \xi < 1 \qquad (4.14)$$

which is equivalent to

$$x = -\frac{1}{\pi} \int_{\xi}^{1} \frac{1}{\tau} \left(\frac{1}{\sqrt{k}} + \left[\sqrt{\frac{1-\tau}{k-\tau}} - \frac{1}{\sqrt{k}} \right] \right) d\tau \quad \text{for } 0 < \xi < 1.$$

Then consider the integral (4.14) as $\xi \to 0^+$ *i.e.* consider the values of x on CD as $\xi \to 0^+$,

$$x \sim \frac{\delta}{\pi} \ln|\xi| - \frac{\delta(1-k)}{\pi} \int_{0}^{1} \frac{d\tau}{\sqrt{k-\tau}(\sqrt{k-k\tau} + \sqrt{k-\tau})}$$

and using (4.2). Hence

$$\Re(B_0) = -\frac{\delta(1-k)}{\pi} \int_{0}^{1} \frac{1}{\sqrt{k-\tau}(\sqrt{k-k\tau} + \sqrt{k-\tau})}. \qquad (4.15)$$

Therefore we can evaluate the integral in (4.15) to obtain $\Re(B_0)$ as a function of δ, and then solve equation (4.13) in ξ_0 with this known $\Re(B_0)$. Hence x values on AB can be evaluated with the initial condition ξ_0 for any δ with a numerical routine in both positive and negative x-direction.

4.1.2. BVP in the Mapped Plane and Velocity Profiles

So far we have stated the relation between the points on the boundary of the flow region and the points on the boundary of the lower-half plane. Now, we will consider the BVP in Fig. 4.2 in the lower half plane. We know that $dw_1/dz = u_1 - iv_1$ is analytic in the flow region and the relation between u_1, v_1 and Q gives $-Q_x + iQ_y$ is also analytic. Therefore to obtain the velocities, it is better to take derivatives of Q in Fig.4.2 with respect to suitable coordinate variables. After taking the derivatives we obtain Fig. 4.6 where $Q_x - iQ_y = W(z)$ is analytic in the flow region.
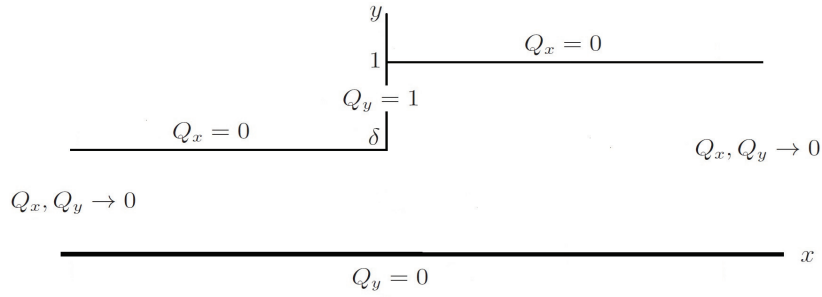
Figure 4.6. Initial Flow Region with the Derivatives of Q

The transformation of this problem onto the lower half plane with the mapping $z = Z(\zeta)$ is shown in Fig. 4.7 where $W(Z(\zeta)) = w(\zeta)$ is analytic in $\eta < 0$, $w(\zeta) \to 0$ as $\zeta \to \infty$ can be written

$$W(z) = W(Z(\zeta)) = w(\zeta) = u + iv = Q_x(X(\xi, \eta), Y(\xi, \eta)) - iQ_y(X(\xi, \eta), Y(\xi, \eta)).$$

We know $w(\zeta)$ is finite at $\xi = 0$ and $\xi = k$ but singular at $\xi = 1$. So we choose a function R such that

$$R(\zeta) = \sqrt{\frac{\zeta - 1}{(\zeta - k)\zeta}}.$$

Then consider the better behaviour of the new function defined by $\tilde{w}(\zeta) = w(\zeta)R(\zeta)$ as
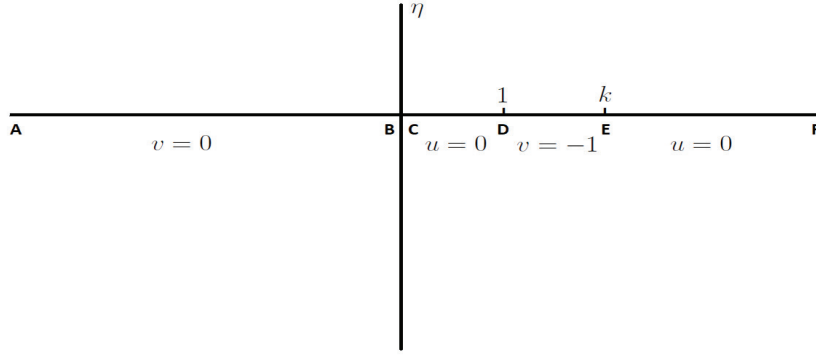
Figure 4.7. Transformation of the problem from the z-plane to the lower half of the ζ
plane

$\zeta \to \infty$. By the equation (4.1), we have

$$x \sim \frac{1}{\pi}\ln\xi \quad \text{as } \zeta \to \infty, \quad i.e. \quad e^{\pi x} \sim \xi \quad \text{as } \zeta \to \infty. \tag{4.16}$$

Then the series solution of p_0 (2.24-2.25) and (4.16) gives,

$$Q \sim \frac{1}{\sqrt{\xi}} \quad \text{as } \zeta \to \infty.$$

By this behaviour of Q, we have

$$Q + i\psi \sim \frac{1}{\sqrt{\zeta}} \quad \text{as } \zeta \to \infty \text{ and then}$$

$$Q_x - iQ_y \sim \frac{d}{dz}\left(\frac{1}{\sqrt{\zeta}}\right) = -\frac{1}{2}\zeta^{-3/2}\frac{d\zeta}{dz} = -\frac{\pi}{2}\frac{1}{\sqrt{\zeta}} \quad \text{as } \zeta \to \infty.$$

So that $\tilde{w}$ behaves $O(1/\zeta)$ as $\zeta \to \infty$. The square roots in R are considered in each
interval as we did for (4.3). Then we see that $\Re[\tilde{w}(\xi - i0)] = -\sqrt{\dfrac{\xi - 1}{(k - \xi)\xi}}$ on the
interval $1 < \xi < k$ and zero on the rest of the boundary. Hence the solution of this

40

BVP-AF can be written as

$$\tilde{w}(\zeta) = -\frac{i}{\pi} \int_1^k \left(\frac{\tau - 1}{(k - \tau)\tau}\right)^{1/2} \frac{d\tau}{\tau - \zeta} \tag{4.17}$$

and $\tilde{w}(\zeta) = O(1/\zeta)$ as $\zeta \to \infty$ which we showed before. The integral in (4.17) can be rewritten by using *Sokhotski-Plemelj Formula* (see Appendix C) on the boundary such that

$$\int_1^k \left(\frac{\tau - 1}{(k - \tau)\tau}\right)^{1/2} \frac{d\tau}{\tau - \xi} =$$
$$\begin{cases} -\dfrac{i}{\pi}\sqrt{\dfrac{\xi - 1}{(k - \xi)\xi}} + P.v. \displaystyle\int_1^k \left(\dfrac{\tau - 1}{(k - \tau)\tau}\right)^{1/2} \dfrac{d\tau}{\tau - \xi}, & 1 < \xi < k, \\[4mm] \displaystyle\int_1^k \left(\dfrac{\tau - 1}{(k - \tau)\tau}\right)^{1/2} \dfrac{d\tau}{\tau - \zeta}, & \xi < 1, \quad \xi > k. \end{cases}$$

To evaluate this integral we consider it in two separate terms such that,

$$\begin{aligned} \int_1^k \left(\frac{\tau - 1}{(k - \tau)\tau}\right)^{1/2} \frac{d\tau}{\tau - \xi} &= \int_1^k \frac{d\tau}{\sqrt{\tau(\tau - 1)(k - \tau)}} \\ &+ (\xi - 1) \int_1^k \frac{d\tau}{(\tau - \xi)\sqrt{\tau(\tau - 1)(k - \tau)}} \\ &= I_1 + (\xi - 1)I_2. \end{aligned} \tag{4.18}$$

For the integral I_1, we use a formula from Gradshteyn&Ryzhik (see Appendix),

$$\begin{aligned} I_1 &= \frac{2}{\sqrt{k}} F(\frac{\pi}{2}, \sqrt{\frac{k - 1}{k}}) \\ &= 2\delta F(\frac{\pi}{2}, \sqrt{1 - \delta^2}) \\ &= 2\delta K(\sqrt{1 - \delta^2}), \end{aligned}$$

where F is the elliptic integral of first kind, K is the complete elliptic integral of first kind

and defined as

$$F(\beta, m) = \int_0^\beta \frac{d\alpha}{\sqrt{1 - m^2 \sin^2 \alpha}}$$

and

$$F(\frac{\pi}{2}, m) = K(m).$$

For the integral I_2 in (4.18), we use another formula from Gradshteyn&Ryzhik (see Appendix),

$$
\begin{aligned}
I_2 &= \frac{2}{\xi(1-\xi)\sqrt{k}} \left[\Pi(\frac{\pi}{2}, \frac{k-1}{k} \frac{\xi}{\xi-1}, \sqrt{\frac{k-1}{k}}) + (\xi-1)F(\frac{\pi}{2}, \sqrt{\frac{k-1}{k}}) \right] \\
&= \frac{2\delta}{\xi(1-\xi)} \left[\Pi(\frac{\pi}{2}, \frac{(1-\delta^2)\xi}{\xi-1}, \sqrt{1-\delta^2}) + (\xi-1)F(\frac{\pi}{2}, \sqrt{1-\delta^2}) \right] \\
&= \frac{2\delta}{\xi(1-\xi)} \left[\bar{\Pi}(\frac{(1-\delta^2)\xi}{\xi-1}, \sqrt{1-\delta^2}) + (\xi-1)\mathbf{K}(\sqrt{1-\delta^2}) \right],
\end{aligned}
$$

where Π is the elliptic integral of third kind, $\bar{\Pi}$ is the complete elliptic integral of third kind, defined as

$$\Pi(\beta, n, m) = \int_0^\beta \frac{d\alpha}{(1 - n \sin^2 \alpha)\sqrt{1 - m^2 \sin^2 \alpha}}$$

and

$$\Pi(\frac{\pi}{2}, n, m) = \bar{\Pi}(n, m).$$

Hence the integral in (4.18) can be written as

$$\int_1^k \left(\frac{\tau - 1}{(k-\tau)\tau} \right)^{1/2} \frac{d\tau}{\tau - \xi} = \frac{2\delta}{\xi} \left[K(\sqrt{1-\delta^2}) - \bar{\Pi}\left(\frac{(1-\delta^2)\xi}{\xi-1}, \sqrt{1-\delta^2} \right) \right].$$

Note that the calculations which we used for the integral (4.18) are valid for $\xi \neq 1$, so we must only consider the behaviour of this integral as $\xi \to 1^+$ for its *principal value* or we can evaluate it for $1 < \xi < k$ with the following way,

$$
P.v. \int_1^k \left(\frac{\tau(\tau - 1)}{(k - \tau)} \right)^{1/2} \frac{d\tau}{\tau - \xi}
$$
$$
= \int_1^k \frac{d\tau}{\sqrt{(\tau - 1)(k - \tau)\tau}} + (\xi - 1)P.v. \int_1^k \frac{d\tau}{(\tau - \xi)\sqrt{(\tau - 1)(k - \tau)\tau}}
$$

and

$$
P.v. \int_1^k \frac{d\tau}{(\tau - \xi)\sqrt{(\tau - 1)(k - \tau)\tau}}
$$
$$
= P.v. \int_1^k \frac{1}{(\tau - \xi)\sqrt{(\tau - 1)(k - \tau)}} \left(\left[\frac{1}{\sqrt{\tau}} - \frac{1}{\sqrt{\xi}} \right] + \frac{1}{\sqrt{\xi}} \right) d\tau
$$
$$
= -\int_1^k \frac{1}{\sqrt{(\tau - 1)(k - \tau)}} \frac{d\tau}{\sqrt{\tau}\sqrt{\xi}(\sqrt{\xi} + \sqrt{\tau})}) + P.v. \frac{1}{\xi} \int_1^k \frac{d\tau}{(\tau - \xi)\sqrt{(\tau - 1)(k - \tau)}}.
$$

Hence,

$$
P.v. \int_1^k \left(\frac{\tau - 1}{(k - \tau)\tau} \right)^{1/2} \frac{d\tau}{\tau - \xi}
$$
$$
= \int_1^k \frac{d\tau}{\sqrt{\tau(\tau - 1)(k - \tau)}} - (\xi - 1) \int_1^k \frac{d\tau}{\sqrt{(\tau - 1)(k - \tau)\tau}\sqrt{\tau}\sqrt{\xi}(\sqrt{\tau} + \sqrt{\xi})}.
$$
$$
= I_1 + (1 - \xi)I_3
$$

It is better to evaluate the integral I_3 numerically.

Since we calculated $\tilde{w}(\zeta)$ on the boundary of the lower half plane, we can obtain $w(\zeta) = \tilde{w}(\zeta)/R(\zeta)$ by considering the behaviour of the square root in $R(\zeta)$ on the boundary. Using the solutions in (4.19) we can obtain Q_x and Q_y on the boundary. Recall the relation $Q = P_0 + y - 1$ and the leading order velocities are $u_1 = -P_{0,x}$, $v_1 = -P_{0,y} - 1$ (see (2.18-2.19)). Thus we can write the leading order velocities as $u_1 = -Q_x$ and $v_1 = -Q_y$.

$$
w(\zeta) \;=\; \begin{cases} \dfrac{1}{\pi}\sqrt{\dfrac{(\xi-k)\xi}{(1-\xi)}}\displaystyle\int_{1}^{k}\left(\dfrac{\tau-1}{(k-\tau)\tau}\right)^{1/2}\dfrac{d\tau}{\tau-\xi} & -\infty<\xi<0,\quad \eta=0 \quad (\text{on } AB), \\[20pt] \dfrac{i}{\pi}\sqrt{\dfrac{(k-\xi)\xi}{(1-\xi)}}\displaystyle\int_{1}^{k}\left(\dfrac{\tau-1}{(k-\tau)\tau}\right)^{1/2}\dfrac{d\tau}{\tau-\xi} & 0<\xi<1,\quad \eta=0 \quad (\text{on } CD), \\[20pt] -i+\dfrac{1}{\pi}\sqrt{\dfrac{(k-\xi)\xi}{(\xi-1)}}P.v.\displaystyle\int_{1}^{k}\left(\dfrac{\tau-1}{(k-\tau)\tau}\right)^{1/2}\dfrac{d\tau}{\tau-\xi} & 1<\xi<k,\quad \eta=0 \quad (\text{on } DE), \\[20pt] \dfrac{i}{\pi}\sqrt{\dfrac{(\xi-k)\xi}{(\xi-1)}}\displaystyle\int_{1}^{k}\left(\dfrac{\tau-1}{(k-\tau)\tau}\right)^{1/2}\dfrac{d\tau}{\tau-\xi} & k<\xi<\infty,\quad \eta=0 \quad (\text{on } EF). \end{cases}
\tag{4.19}
$$

Hence we can calculate the horizontal velocity $u_1(x)$ at the bottom $y=0$ by using the following formula and the values of x are evaluated numerically,

$$
u_1(\xi) = -\frac{1}{\pi}\sqrt{\frac{(\xi-k)\xi}{1-\xi}}\int_{1}^{k}\left(\frac{\tau-1}{(k-\tau)\tau}\right)^{1/2}\frac{d\tau}{\tau-\xi}\qquad -\infty<\xi<0.
$$

The Fig. 4.8 shows horizontal velocity profile for different values of δ.
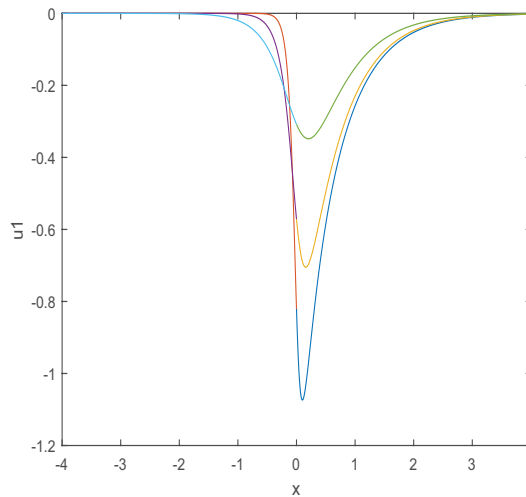
Figure 4.8. Horizontal velocity in terms of x. From top to bottom $\delta=\frac{1}{2},\frac{1}{4},\frac{1}{8}$ (for which $k=4,16,64$, respectively)

We depict the horizontal velocity $u_1(y)$ of the initially vertical free surface (on DE) by using the following formulas,

$$
\begin{aligned}
u_1(\xi) &= \frac{1}{\pi}\sqrt{\frac{(k-\xi)\xi}{\xi-1}}P.v.\int_1^k \left(\frac{\tau-1}{(k-\tau)\tau}\right)^{1/2}\frac{d\tau}{\tau-\xi} \\
y(\xi) &= \delta + \frac{1}{\pi}\int_1^\xi \frac{1}{\tau}\sqrt{\frac{\tau-1}{k-\tau}}d\tau, \quad 1 < \xi < k
\end{aligned}
$$

for $\delta = 1/2$ in Fig. 4.9. Note u_1 is singular at $y = \delta = 0.5$

The vertical velocity $v_1(x)$ on EF defined as

$$
\begin{aligned}
v_1(\xi) &= \frac{1}{\pi}\sqrt{\frac{(\xi-k)\xi}{\xi-1}}\int_1^k \left(\frac{\tau-1}{(k-\tau)\tau}\right)^{1/2}\frac{d\tau}{\tau-\xi} \\
x(\xi) &= \frac{1}{\pi}\int_k^\xi \frac{1}{\tau}\sqrt{\frac{\tau-1}{\tau-k}}d\tau, \quad k < \xi < \infty.
\end{aligned}
$$
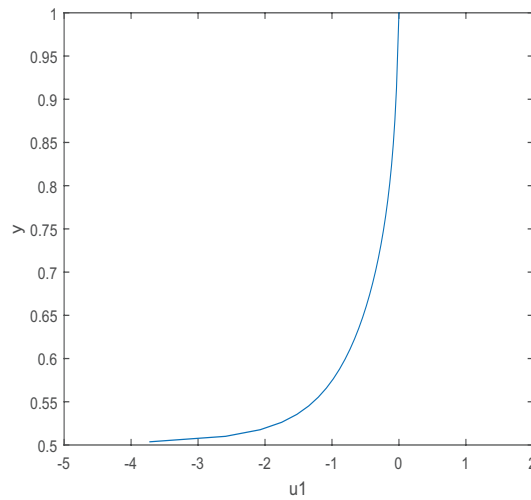
Figure 4.9. Horizontal velocity in terms of y on the vertical free surface.

The vertical velocity as a function of x is shown for $\delta = 1/2$ in Fig. 4.10, Then,
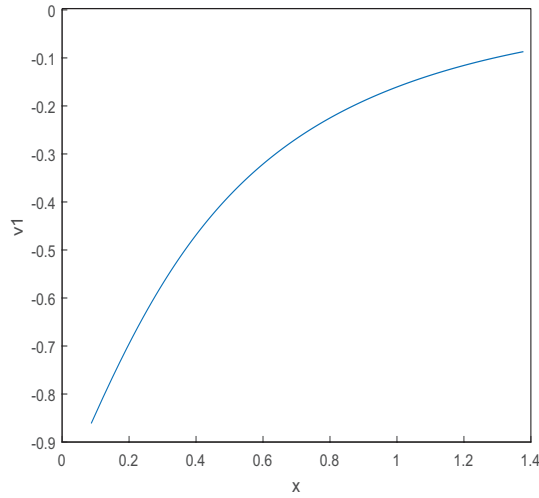
Figure 4.10. Veritical velocity at $y = 1$ in terms of x

the vertical velocity $v_1(x)$ on CD is

$$v_1(\xi) = \frac{1}{\pi} \sqrt{\frac{(k - \xi)\xi}{1 - \xi}} \int_1^k \left(\frac{\tau - 1}{(k - \tau)\tau} \right)^{1/2} \frac{d\tau}{\tau - \xi},$$

$$x(\xi) = -\frac{1}{\pi} \int_\xi^1 \frac{1}{\tau} \sqrt{\frac{1 - \tau}{k - \tau}} d\tau, \quad 0 < \xi < 1.$$

$v_1(x)$ is plotted in Fig. 4.11.

Note that v_1 is singular as x increases to zero.

The velocity components (and pressure) are the main items of interact. So, after we finish the sketch of velocity profiles for the boundary, we will continue for the image of the interface at the lower half of ζ plane and seek the velocity profile also at the interface. Therefore we will obtain the velocity profiles at the whole boundary and at the interface.

First consider the image of the interface ($x = 0$, $0 < y < \delta$) on the ζ-plane. Integrating (4.3) from $\xi = 1$ gives

$$Z(\zeta) - i\delta = \frac{1}{\pi} \int_1^\zeta \frac{1}{\tau} \sqrt{\frac{\tau - 1}{\tau - k}} d\tau,$$
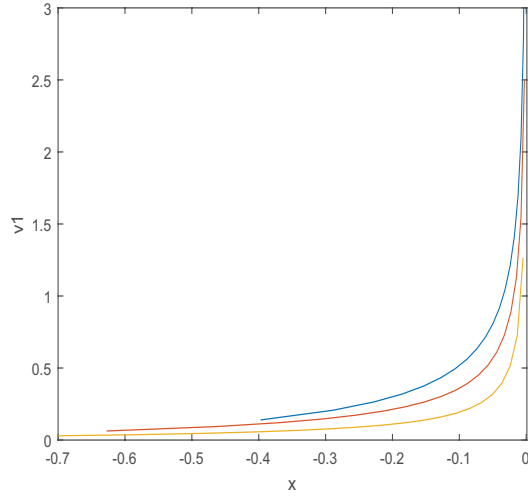
Figure 4.11. Veritical velocity in terms of x. From left to right the curves are $\delta = 0.5, 0.75, 0.9$

where $\zeta = \zeta(y)$, y is considered as a curvilinear coordinate along the image of the interface. On the interface, $dZ = idy$ and (4.3) gives

$$\frac{idy}{d\zeta} = \frac{1}{\pi\zeta}\sqrt{\frac{\zeta - 1}{\zeta - k}}.$$

Then

$$\begin{cases} \dfrac{d\zeta}{dy} = \pi i\zeta\sqrt{\dfrac{\zeta - k}{\zeta - 1}} & (0 < y < \delta), \\ \zeta(\delta) = 1. \end{cases} \tag{4.20}$$

Equation (4.20) can be integrated with y varying from δ to 0. Note that the right hand side of the equation (4.20) is singular at $y = \delta$. We introduce a new variable τ as $y = \delta(1 - \tau)$, so that $dy = -\delta d\tau$ where τ varies from 0 to 1 along the interface. Then $\zeta = 1 + r(\tau)e^{\alpha(\tau)}$ (see (4.4)) and let $(\zeta - 1)^{3/2} = \varpi$ where $\varpi = \mid \varpi \mid e^{i\Omega}$ and

47

$\varpi = \lambda(\tau) + i\mu(\tau)$. Now,

$$
\begin{aligned}
\frac{d\varpi}{d\tau} &= \frac{d\varpi}{dy}\frac{dy}{d\tau} = -\delta\frac{d\varpi}{dy} \\
&= -\delta\frac{3}{2}(\zeta - 1)^{1/2}\frac{d\zeta}{dy} \\
&= -\frac{3}{2}\delta\pi i\zeta(\zeta - k)^{1/2}
\end{aligned}
$$

where $\zeta = k + \rho(\tau)e^{i\beta(\tau)}$ (see (4.5)). Next,

$$
\begin{aligned}
\frac{d\varpi}{d\tau} &= \frac{d\lambda}{d\tau} + i\frac{d\mu}{d\tau} \\
&= -\frac{3}{2}\pi\delta i(k + \rho e^{i\beta})\sqrt{\rho}e^{i\beta/2}
\end{aligned}
$$

which gives

$$
\left.
\begin{aligned}
\frac{d\lambda}{d\tau} &= \frac{3}{2}\pi\delta\sqrt{\rho}\left(k\sin\left(\frac{\beta}{2}\right) + \rho\sin\left(\frac{3\beta}{2}\right)\right) \\
\frac{d\mu}{d\tau} &= -\frac{3}{2}\pi\delta\sqrt{\rho}\left(k\cos\left(\frac{\beta}{2}\right) + \rho\cos\left(\frac{3\beta}{2}\right)\right) \\
&\text{where } 0 < \tau < 1 \text{ and } \lambda(0) = 0,\ \mu(0) = 0
\end{aligned}
\right\}
\tag{4.21}
$$

[on the domain's boundary β=0 or $\beta = -\pi$]. The right hand side of the equations (4.21) is calculated using $\lambda(\tau)$ and $\mu(\tau)$ as it is regular now. Since $(\zeta - 1)^{3/2} = \mid \varpi \mid e^{i\Omega}$,

$$
\zeta = 1 + |\varpi|^{\frac{2}{3}}e^{i\frac{2\Omega}{3}} = k + \rho(\tau)e^{i\beta(\tau)}
$$

and we get a relation between $\lambda(\tau)$, $\mu(\tau)$ and $\rho(\tau)$, $\beta(\tau)$ such that

$$
\begin{aligned}
1 + |\varpi|^{2/3}\cos(\frac{2\Omega}{3}) &= k + \rho(\tau)\cos(\beta(\tau)) \\
|\varpi|^{2/3}\sin(\frac{2\Omega}{3}) &= \rho(\tau)\sin(\beta(\tau))
\end{aligned}
$$

which gives,

$$\rho(\tau) = \left(\left(1 - k + |\varpi|^{2/3}\cos(\frac{2\Omega}{3})\right)^2 + \left(|\varpi|^{2/3}\sin(\frac{2\Omega}{3})\right)^2\right)^{1/2}$$

$$\beta(\tau) = \arctan\left(\frac{|\varpi|^{2/3}\sin(\frac{2\Omega}{3})}{1 - k + |\varpi|^{2/3}\cos(\frac{2\Omega}{3})}\right) \qquad 0 < \tau < 1,$$

where

$$|\varpi|^{2/3} = (\lambda(\tau)^2 + \mu(\tau)^2)^{1/3} \quad \text{and} \quad \Omega(\tau) = \arctan\left(\frac{\mu(\tau)}{\lambda(\tau)}\right): \quad -3\pi/2 < \Omega < 0,$$

Ω should be calculated carefully for given λ, μ.

Solution of (4.21) with adaptive step-size Runge-Kutta method gives the following shape of the interface $\zeta(y)$ for $\delta = \frac{1}{2}, \frac{1}{4}, \frac{1}{8}$ Fig. 4.12,
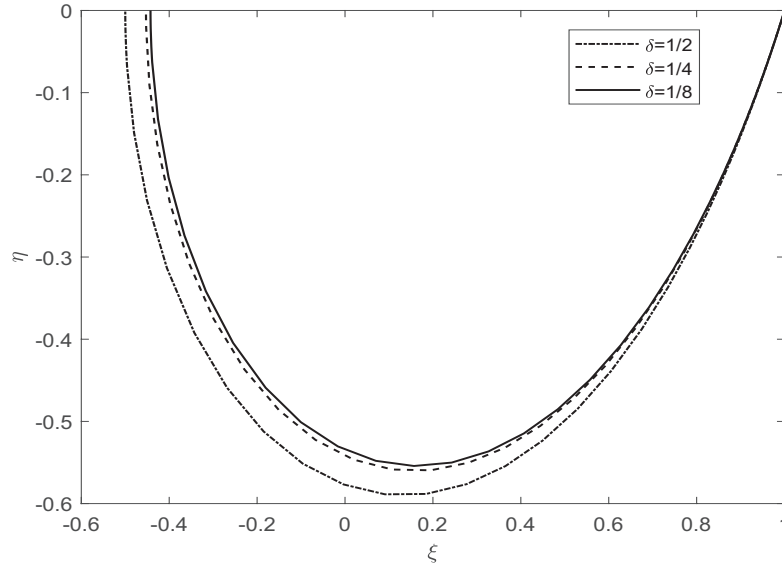
Figure 4.12. Shape of the interface $\zeta(y)$ for $\delta = \frac{1}{2}, \frac{1}{4}, \frac{1}{8}$

4.2. Asymptotic Analysis of the Velocity Near Corner Point

We know the velocity is singular at the corner point $(0, \delta)$, so we can analyze the vertical velocity on CD and the horizontal velocity on DE near the corner point to obtain the order of the singularity and the coefficient of the singularity. Since we know the values of $v_1(\xi)$ and $x(\xi)$ on CD, we start with the analysis of $x(\xi)$ as $\xi \to 1 - 0$ i.e. $\xi = 1 - \varepsilon$ where $0 < \varepsilon \ll 1$. Since

$$x(\xi) = -\frac{1}{\pi} \int_\xi^1 \frac{1}{\tau} \sqrt{\frac{1 - \tau}{k - \tau}} d\tau, \quad 0 < \xi < 1,$$

we can write

$$
\begin{aligned}
x(\varepsilon) &= -\frac{1}{\pi} \int_{1-\varepsilon}^1 \frac{1}{\tau} \sqrt{\frac{1 - \tau}{k - \tau}} d\tau \quad \text{and by the change of variables } \tau = 1 - \varepsilon\sigma, \\
&= -\frac{1}{\pi} \varepsilon^{3/2} \int_0^1 \frac{\sigma^{1/2}}{\sqrt{k - 1 + \varepsilon\sigma}(1 - \varepsilon\sigma)} d\sigma.
\end{aligned}
$$

The Taylor series expansions in powers of ε of the two terms are

$$
\begin{aligned}
\frac{1}{1 - \varepsilon\sigma} &= 1 + \varepsilon\sigma + O(\varepsilon^2) \quad \text{and} \\
\frac{1}{\sqrt{k - 1 + \varepsilon\sigma}} &= \frac{1}{\sqrt{k - 1}}\left(1 - \frac{1}{2}\frac{\varepsilon\sigma}{k - 1} + O(\varepsilon^2)\right).
\end{aligned}
$$

This shows that on CD x depends on ε as follows:

$$x(\varepsilon) = \varepsilon^{3/2} H_1(\varepsilon) \quad \text{for } 0 < \varepsilon \ll 1, \tag{4.22}$$

where

$$H_1(\varepsilon) = -\frac{2}{3\pi}(k - 1)^{-1/2} - \frac{2}{5\pi}\frac{2k - 3}{2k - 2}(k - 1)^{-1/2}\varepsilon + O(\varepsilon^2).$$

Similarly, we can analyze $v_1(\xi)$ on CD as $\xi \to 1 - 0$ and we let $\xi = 1 - \varepsilon$ where $0 < \varepsilon \ll 1$. Hence

$$v_1(\xi) = \frac{1}{\pi}\sqrt{\frac{(k-\xi)\xi}{1-\xi}}\int_1^k \left(\frac{\tau-1}{(k-\tau)\tau}\right)^{1/2}\frac{d\tau}{\tau-\xi}, \quad 0 < \xi < 1. \qquad (4.23)$$

We now analyze (4.23) by simplifying the integral in $v_1(\xi)$,

$$
\begin{aligned}
\int_1^k \left(\frac{\tau-1}{(k-\tau)\tau}\right)^{1/2}\frac{d\tau}{\tau-\xi} &= \int_1^k \sqrt{\frac{\tau-1}{(k-\tau)}}\left(\frac{1}{\sqrt{\xi}} + \left[\frac{1}{\sqrt{\tau}} - \frac{1}{\sqrt{\xi}}\right]\right)\frac{d\tau}{\tau-\xi} \\
&= \frac{1}{\sqrt{\xi}}\int_1^k \sqrt{\frac{\tau-1}{(k-\tau)}}\frac{d\tau}{\tau-\xi} \\
&\quad - \frac{1}{\sqrt{\xi}}\int_1^k \sqrt{\frac{\tau-1}{(k-\tau)}}\frac{d\tau}{\sqrt{\tau}(\sqrt{\xi}+\sqrt{\tau})} \\
&= \frac{1}{\sqrt{\xi}}(I_1 - I_2).
\end{aligned}
$$

The integral I_2 can be expanded using Taylor series by putting $\xi = 1-\varepsilon$ where $0 < \varepsilon \ll 1$ and letting

$$I_2 = \sum_{n=0}^{\infty} a_n \varepsilon^n.$$

On the other hand

$$
\begin{aligned}
I_1 &= \int_1^k \frac{\tau-1}{\tau-\xi}\frac{d\tau}{\sqrt{(k-\tau)(\tau-1)}} \\
&= \int_1^k \left(1 + \frac{\xi-1}{\tau-\xi}\right)\frac{d\tau}{\sqrt{(k-\tau)(\tau-1)}} \\
&= \pi + (\xi-1)\int_1^k \frac{d\tau}{(\tau-\xi)\sqrt{(k-\tau)(\tau-1)}}.
\end{aligned}
$$

By the change of variable $\tau = \dfrac{(k-1)\lambda + (k+1)}{2}$,

$$I_1 = \pi + (\xi - 1)\frac{2}{k-1}\frac{\pi}{\sqrt{\left(\frac{2(\xi-1)}{k-1} - 1\right)^2 - 1}}$$

$$= \pi + (\xi - 1)\frac{\pi}{\sqrt{1-\xi}\sqrt{k-\xi}}. \qquad (4.24)$$

Then $v_1(\xi)$ on CD as $\xi \to 1 - 0$ *i.e.* $\xi = 1 - \varepsilon$ where $0 < \varepsilon \ll 1$ becomes

$$v_1(\xi) \sim \frac{1}{\pi}\sqrt{\frac{k-\xi}{1-\xi}}\left(\pi + (\xi-1)\frac{\pi}{\sqrt{1-\xi}\sqrt{k-\xi}} - \sum_{n=0}^{\infty} a_n \varepsilon^n\right)$$

$$\sim -1 + \sqrt{\frac{k-\xi}{1-\xi}}\left(1 - \frac{1}{\pi}\sum_{n=0}^{\infty} a_n \varepsilon^n\right)$$

$$= -1 + \sqrt{\varepsilon}\sqrt{k-1}\left(1 + \frac{\varepsilon}{k-1}\right)^{1/2}\left(1 - \frac{1}{\pi}\sum_{n=0}^{\infty} a_n \varepsilon^n\right).$$

The Taylor series expansion of the term

$$\left(1 + \frac{\varepsilon}{k-1}\right)^{1/2} = 1 + \frac{\varepsilon}{2(k-1)} + O(\varepsilon^2)$$

gives the analysis of the vertical velocity v_1 on CD such that

$$v_1(\varepsilon) = -1 + \varepsilon^{-1/2}G_1(\varepsilon), \qquad (4.25)$$

where

$$G_1(\varepsilon) = \left(1 - \frac{a_0}{\pi}\right)(k-1)^{1/2} + \left[\frac{1}{2}(1 - \frac{a_0}{\pi})(k-1)^{-1/2} - \frac{a_1}{\pi}(k-1)^{1/2}\right]\varepsilon + O(\varepsilon^2)$$

and

$$a_0 = \pi - 2\delta F(1 - \delta^2) \quad \text{and} \quad a_1 = \frac{\delta(1+\delta^2)}{1-\delta^2}F(1-\delta^2) - \frac{\delta^3}{1-\delta^2}E(1-\delta^2).$$

Since we need the expansion of the vertical velocity v_1 in terms of x, we will make some re-arrangements. By using (4.22), we have $\varepsilon^{-1/2} = x^{-1/3}H_1^{1/3}(\varepsilon)$ which gives

$$v_1(\varepsilon) = -1 + x^{-1/3}\tilde{G}_1(\varepsilon), \quad (\tilde{G}_1(\varepsilon) = G_1(\varepsilon)H_1^{1/3}(\varepsilon)), \tag{4.26}$$

and

$$
\begin{aligned}
\tilde{G}_1(\varepsilon) &= \left(-\frac{2}{3}\right)^{1/3}\frac{\pi - a_0}{\pi^{4/3}}(k-1)^{1/3} \\
&+ \left(-\frac{2}{3}\right)^{1/3}\frac{(k+1)(\pi - a_0) - 5a_1(k-1)}{5\pi^{4/3}}(k-1)^{-2/3}\varepsilon + O(\varepsilon^2).
\end{aligned}
$$

On the other hand, by the inversion of the power series, the relation $x^{2/3} = \varepsilon H_1^{2/3}(\varepsilon)$ obtained from (4.22) gives

$$\varepsilon = -\left(\frac{3\pi}{2}\right)^{2/3}(k-1)^{1/3}x^{2/3} + \frac{3-2k}{5}\left(\frac{3\pi}{2}\right)^{4/3}(k-1)^{-1/3}x^{4/3} + \cdots. \tag{4.27}$$

Substituting (4.27) into (4.26) gives that the leading order vertical velocity v_1 is singular of order $-\frac{1}{3}$ near the corner point and the coefficient of the singularity is calculated as

$$v_1 = -1 - \frac{2\delta F(1-\delta^2)}{\pi^{4/3}}\left(\frac{2}{3}\right)^{1/3}(k-1)^{1/3}x^{-1/3} + O(x^{1/3}). \tag{4.28}$$

We will do the same steps for the analysis of the leading order horizontal velocity $u_1(\xi)$ and $y(\xi)$ on DE. We start with the analysis of $y(\xi)$ by approaching as $\xi \to 1+0$ i.e. $\xi = 1 + \varepsilon$ where $0 < \varepsilon \ll 1$. Since

$$y(\xi) = \delta + \frac{1}{\pi}\int_1^\xi \frac{1}{\tau}\sqrt{\frac{\tau - 1}{k - \tau}}d\tau, \quad 1 < \xi < k.$$

We can write

$$
\begin{aligned}
y(\varepsilon) &= \delta + \frac{1}{\pi} \int_1^{1+\varepsilon} \frac{1}{\tau} \sqrt{\frac{\tau-1}{k-\tau}} \, d\tau, \quad \text{and by the change of variables } \tau = 1 + \varepsilon\sigma \\
&= \delta + \frac{1}{\pi} \varepsilon^{3/2} \int_0^1 \frac{\sigma^{1/2}}{\sqrt{k-1-\varepsilon\sigma}(1+\varepsilon\sigma)} \, d\sigma.
\end{aligned}
$$

The Taylor series expansions in powers of ε of the two terms are

$$
\begin{aligned}
\frac{1}{1+\varepsilon\sigma} &= 1 - \varepsilon\sigma + O(\varepsilon^2) \quad \text{and} \\
\frac{1}{\sqrt{k-1-\varepsilon\sigma}} &= \frac{1}{\sqrt{k-1}}\left(1 + \frac{1}{2}\frac{\varepsilon\sigma}{k-1} + O(\varepsilon^2)\right).
\end{aligned}
$$

Therefore on DE is

$$
y(\varepsilon) = \delta + \varepsilon^{3/2} H_2(\varepsilon) \tag{4.29}
$$

where

$$
H_2(\varepsilon) = \frac{2}{3\pi}(k-1)^{-1/2} - \frac{2}{5\pi}\frac{2k-3}{2k-2}(k-1)^{-1/2}\varepsilon + O(\varepsilon^2).
$$

Similarly, we can analyse $u_1(\xi)$ on DE as $\xi \to 1 + 0$ *i.e.* $\xi = 1 + \varepsilon$ where $0 < \varepsilon \ll 1$. Since

$$
u_1(\xi) = -\frac{1}{\pi}\sqrt{\frac{(k-\xi)\xi}{\xi-1}} P.v. \int_1^k \left(\frac{\tau-1}{(k-\tau)\tau}\right)^{1/2} \frac{d\tau}{\tau-\xi}, \quad 1 < \xi < k,
$$

we start by simplifying the *Principal value* integral in $u_1(\xi)$,

$$
\begin{aligned}
&P.v. \int_1^k \left(\frac{\tau-1}{(k-\tau)\tau}\right)^{1/2} \frac{d\tau}{\tau-\xi} \\
&= P.v. \int_1^k \sqrt{\frac{\tau-1}{(k-\tau)}}\left(\frac{1}{\sqrt{\xi}} + \left[\frac{1}{\sqrt{\tau}} - \frac{1}{\sqrt{\xi}}\right]\right)\frac{d\tau}{\tau-\xi} \\
&= \frac{1}{\sqrt{\xi}} P.v. \int_1^k \sqrt{\frac{\tau-1}{k-\tau}}\frac{d\tau}{\tau-\xi} - \frac{1}{\sqrt{\xi}}\int_1^k \sqrt{\frac{\tau-1}{k-\tau}}\frac{d\tau}{\sqrt{\tau}(\xi+\tau)}
\end{aligned}
$$

54

$$= \frac{1}{\sqrt{\xi}}(I_3 - I_4).$$

The integral I_4 can be expanded into Taylor series for $\xi = 1 + \varepsilon$ where $0 < \varepsilon \ll 1$ and let

$$I_4 = \sum_{n=0}^{\infty} b_n \varepsilon^n.$$

On the other hand

$$
\begin{aligned}
I_3 &= P.v. \int_1^k \left(1 + \frac{\xi - 1}{\tau - \xi}\right) \frac{d\tau}{(k - \tau)(\tau - 1)} \\
&= \int_1^k \frac{d\tau}{(k - \tau)(\tau - 1)} + (\xi - 1)P.v. \int_1^k \frac{d\tau}{(\tau - \xi)\sqrt{(k - \tau)(\tau - 1)}} \\
&= \pi.
\end{aligned}
$$

Then $u_1(\xi)$ on DE as $\xi \to 1 + 0$ i.e. $\xi = 1 + \varepsilon$ where $0 < \varepsilon \ll 1$ becomes

$$
\begin{aligned}
u_1 &\sim -\frac{1}{\pi}\sqrt{\frac{k - \xi}{\xi - 1}}\left(\pi - \sum_{n=0}^{\infty} b_n \varepsilon^n\right) \\
&= -\sqrt{\varepsilon}\sqrt{k - 1}\left(1 - \frac{\varepsilon}{k - 1}\right)^{1/2}\left(1 - \frac{1}{\pi}\sum_{n=0}^{\infty} b_n \varepsilon^n\right).
\end{aligned}
$$

The Taylor expansion of the term

$$\left(1 - \frac{\varepsilon}{k - 1}\right)^{1/2} = 1 - \frac{\varepsilon}{2(k - 1)} + O(\varepsilon^2)$$

gives the analysis of the horizontal velocity u_1 on DE such that

$$u_1(\varepsilon) = \varepsilon^{-1/2}G_2(\varepsilon) \tag{4.30}$$

where

55

$$G_2(\varepsilon) = \left(\frac{b_0}{\pi} - 1\right)(k-1)^{1/2} + \left[\frac{b_1}{\pi}(k-1)^{1/2} + \frac{1}{2}(1 - \frac{b_0}{\pi})(k-1)^{-1/2}\right]\varepsilon + O(\varepsilon^2),$$

and

$$b_0 = a_0 \quad \text{and} \quad b_1 = -a_1.$$

Since we need the expansion of the horizontal velocity u_1 in terms of y, we will do some arrangements. By using (4.29) we have $\varepsilon^{-1/2} = (y-\delta)^{-1/3}H_2^{1/3}(\varepsilon)$ which gives

$$u_1(\varepsilon) = -1 + x^{-1/3}\tilde{G}_2(\varepsilon), \quad (\tilde{G}_2(\varepsilon) = G_2(\varepsilon)H_2^{1/3}(\varepsilon)), \tag{4.31}$$

and

$$\begin{aligned}
\tilde{G}_2(\varepsilon) &= \left(\frac{2}{3}\right)^{1/3}\frac{b_0 - \pi}{\pi^{4/3}}(k-1)^{1/3} \\
&+ \left(\frac{2}{3}\right)^{1/3}\frac{(k+1)(\pi - b_0) + 5b_1(k-1)}{5\pi^{4/3}}(k-1)^{-2/3}\varepsilon + O(\varepsilon^2).
\end{aligned}$$

On the other hand, by the inversion of the power series $(y-\delta)^{2/3} = \epsilon H_2^{2/3}(\epsilon)$ obtained from (4.29), we get

$$\begin{aligned}
\varepsilon &= \left(\frac{3\pi}{2}\right)^{2/3}(k-1)^{1/3}(y-\delta)^{2/3} \\
&- \frac{3-2k}{5}\left(\frac{3\pi}{2}\right)^{4/3}(k-1)^{-1/3}(y-\delta)^{4/3} + \cdots. \tag{4.32}
\end{aligned}$$

Substituting (4.32) into (4.31) gives that the leading order horizontal velocity u_1 is also singular of order $-\frac{1}{3}$ near the triple point and the coefficient of the singularity is calculated as

$$u_1 = -\frac{2\delta F(1-\delta^2)}{\pi^{4/3}}\left(\frac{2}{3}\right)^{1/3}(k-1)^{1/3}(y-\delta)^{-1/3} + O((y-\delta)^{1/3}) \tag{4.33}$$

56

which is the comparison with Galerkin same as (4.28).

4.3. Comparison of the Velocity at the Interface: Analytical Solution vs. Galerkin Solution

We compare the obtained horizontal velocity profile at the interface with the Galerkin approximation solution which we derived before by using the suitable test function. We see that the Galerkin solution is very close to analytical solution. This comparison makes us sure about the choice of the test function in Galerkin method.
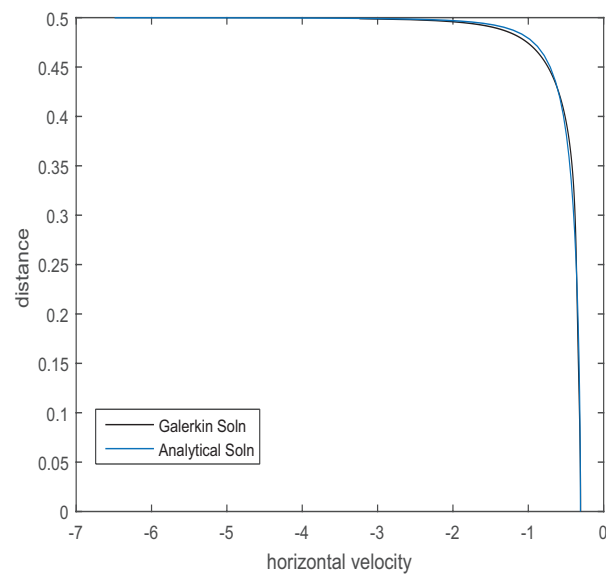
Figure 4.13. Comparison of the horizontal velocity at the interface

CHAPTER 5

SOLUTION BY CONFORMAL MAPPING, SECOND ORDER

The same conformal mapping as used in chapter 4 can be used for the analytical solution of the dam-break problem at the second order. So in this chapter, the second order problem is derived by using the main equations of the problem and small-time expansions of the unknowns stated at Chapter 2. But we encounter with the Poisson equation instead of the Laplace equation at the second order. Thus first we need to change the Poisson equation to the Laplace equation with suitable transformations. Then the solution of the second order problem with an unknown additive constant is obtained.

5.1. Second Order Pressure

At the second order, we have the following boundary value problem

$$
\left.
\begin{aligned}
u_{3,x}^{+} + v_{3,y}^{+} = 0 \quad &\text{in } \Omega^{+}, \\[6pt]
3u_3^{+} + u_1^{+}u_{1,x}^{+} + v_1^{+}u_{1,y}^{+} = -p_{2,x}^{+} \quad &\text{in } \Omega^{+}, \\[6pt]
3v_3^{+} + u_1^{+}v_{1,x}^{+} + v_1^{+}v_{1,y}^{+} = -p_{2,y}^{+} \quad &\text{in } \Omega^{+}, \\[6pt]
v_3^{+}(x,0) = 0\,, \quad p_2^{+}(x,1) = -p_{0,y}^{+}(x,1)\eta_2^{+}\,, \quad p_2^{+}(0,y) = -p_{0,x}^{+}(0,y)\xi_2^{+}, \\[6pt]
4\eta_4^{+} = v_3^{+}(x,1) - u_1^{+}(x,1)\eta_{2,x}^{+} + v_{1,y}^{+}(x,1)\eta_2^{+}, \\[6pt]
4\xi_4^{+} = u_3^{+}(0,y) - v_1^{+}(0,y)\xi_{2,y}^{+} + u_{1,x}^{+}(0,y)\xi_2^{+}
\end{aligned}
\right\}
\tag{5.1}
$$

with $u_3^{+}, v_3^{+} \to 0$ and $p_2^{+} \to 0$ as $x \to \infty$.

$$u_{3,x}^- + v_{3,y}^- = 0 \quad \text{in } \Omega^-,$$

$$3u_3^- + u_1^- u_{1,x}^- + v_1^- u_{1,y}^- = -p_{2,x}^- \quad \text{in } \Omega^-,$$

$$3v_3^- + u_1^- v_{1,x}^- + v_1^- v_{1,y}^- = -p_{2,y}^- \quad \text{in } \Omega^-,$$

$$v_3^-(x,0) = 0, \quad p_2^-(x,\delta) = -p_{0,y}^+(x,\delta)\eta_2^-,$$

$$4\eta_4^- = v_3^-(x,\delta) - u_1^-(x,\delta)\eta_{2,x}^- + v_{1,y}^-(x,\delta)\eta_2^+,$$

$$\left. \right\} \quad (5.2)$$

with $u_3^-, v_3^- \to 0$ and $p_2^- \to 0$ as $x \to \infty$.

The problem (5.1) and (5.2) are equivalent to the boundary value problem

$$\Delta p_2^+ = -2((u_{1,x}^+)^2 + (u_{1,y}^+)^2) \quad \text{in } \Omega^+,$$

$$p_2^+(x,1) = \tfrac{1}{2}v_1^+(v_1^+ + 1), \quad p_2^+(0,y) = \tfrac{1}{2}(u_1^+)^2, \quad p_{2,y}^+(x,0) = 0$$

$$\left. \right\} \quad (5.3)$$

with $p_2^+ \to 0$ as $x \to \infty$.

$$\Delta p_2^- = -2((u_{1,x}^-)^2 + (u_{1,y}^-)^2) \quad \text{in } \Omega^-,$$

$$p_2^-(x,\delta) = \tfrac{1}{2}v_1^-(v_1^- + 1), \quad p_{2,y}^-(x,0) = 0$$

$$\left. \right\} \quad (5.4)$$

with $p_2^- \to 0$ as $x \to \infty$ with the boundary conditions on the interface,

$$(u_{1,x}^+(0,y) - u_{1,x}^-(0,y))b_2(y) + u_3^+(y) - u_3^-(y) = (v_1^+(0,y) - v_1^-(0,y))b_{2,y}(y),$$
$$(\gamma u_1^-(0,y) - u_1^+(0,y))b_2(y) = p_2^+(0,y) - p_2^-(0,y).$$

$$\left. \right\} \quad (5.5)$$

It is hard to solve the problem (5.3) and (5.4) with the interface conditions (5.5) by direct methods. But simplification of the geometry of the problem by using conformal mapping helps us as we did for the leading order problem. Since the second order pressure

is also continuous at the interface when the liquid density is the same on either side, the BVP (5.3)-(5.4) can be written as the following BVP Fig. 5.1,

Figure 5.1. Second order problem

To solve this problem, we first use the transformation $F = p_2 + u_1^2$ to change the Poisson's equation for p_2 in Fig. 5.1 to Laplace equation for F. Fig. 5.2 shows the boundary value problem for F.

Figure 5.2. Second order problem with the unknown function F

To have a Laplace equation for F is good, but getting the solution at the mapped region needs homogeneous boundary conditions at the infinity part of the boundary. So we also need to simplify the boundary condition at the right horizontal free surface. We use the analytic function $dw_1/dz = u_1 - iv_1$ in the flow region and hence $\nu = idw_1/dz$ is also analytic. Therefore we can use the transformation $\tilde{F} = F - \Re(\frac{1}{2}\nu^2)$ to make the

boundary conditions simpler and the BVP in terms of the harmonic function $\tilde{F}$ becomes Fig. 5.3.
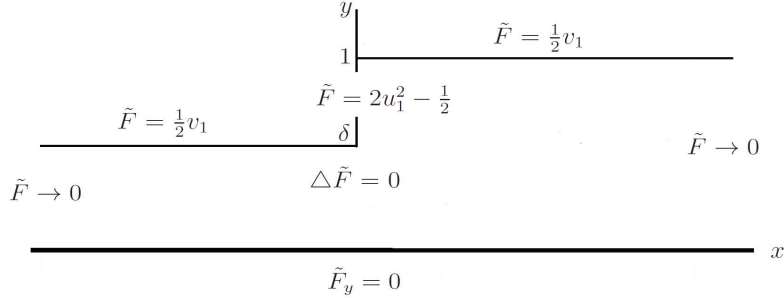
Figure 5.3. Second order problem with the unknown function $\tilde{F}$

But the condition $\tilde{F} = \frac{1}{2}v_1$ on $y = 1$ is still not good enough since that part of the boundary corresponds to infinity part of the boundary in the mapped plane. So we need another transformation to make this condition zero. Let $\bar{W}(z) = \tilde{F} + iG$ be analytic function in the flow region. Define a new analytic function $W_2(z)$ such that

$$W_2(z) = \bar{W}(z) - \frac{i}{2}\frac{dw_1}{dz}(-iz).$$

The real and the imaginary parts of $W_2(z)$ are denoted by $\Re[W_2(z)]$ and $\Im[W_2(z)]$ respectively and satisfy the following conditions on the boundary of the flow region,

$$\Im[W_2(z)] = \Im[W_2(x + i0)] = G - \frac{x}{2}v_1 = 0 \quad \text{on AB}.$$

Since $v_1 = 0$ on AB and $G = 0$ on AB ($\tilde{F}_y = 0$ on AB, since $\tilde{F}$ is harmonic we can use Cauchy-Riemann equations (see Appendix D) and obtain $G_x = 0$ on AB. $G_x = 0$ on AB and $G \to 0$ as $x \to \pm\infty$ together implies that $G = 0$ on AB).

$$\Re[W_2(z)] = \Re[W_2(x + i)] = \tilde{F} - \frac{v_1}{2} = 0 \quad \text{on } EF$$

61

since $u_1 = 0$ and $\tilde{F} = v_1/2$ on EF.

$$\Re[W_2(z)] \;=\; \Re[W_2(x + i\delta)] = \tilde{F} - \frac{\delta}{2}v_1 = \frac{1-\delta}{2}v_1 \quad \text{on } CD$$

since $u_1 = 0$ and $\tilde{F} = v_1/2$ on CD.

$$\Re[W_2(z)] \;=\; \Re[W_2(0 + iy)] = \tilde{F} - \frac{y}{2} = 2u_1^2 + \frac{y-1}{2} \quad \text{on } DE$$

since $v_1 = -1$ and $\tilde{F} = 2u_1^2 - \frac{1}{2}$ on DE. Then the BVP in Fig. 5.3 in terms of the analytic function $W_2(z)$ becomes Fig. 5.4.
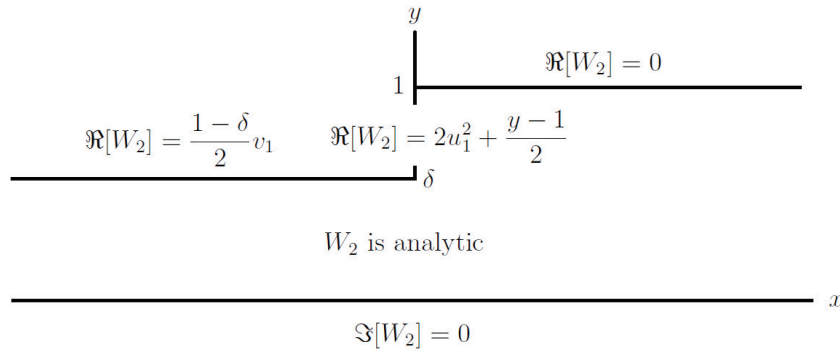
Figure 5.4. Second order problem with the unknown function W_2

We can use the same mapping $z = Z(\zeta)$ (4.3) for the transformation of the BVP Fig. 5.4 onto the lower half plane with Fig. 5.5, where $W_3(\zeta) = W_2[Z(\zeta)]$ is analytic in $\eta < 0$, $W_3 \to 0$ as $\zeta \to \infty$.

We know W_3 is finite at $\xi = 0$ and $\xi = k$ but singular at $\xi = 1$. So we choose a function $\tilde{R}$ such that

$$\tilde{R}(\zeta) = \frac{\zeta - 1}{\sqrt{\zeta}}.$$
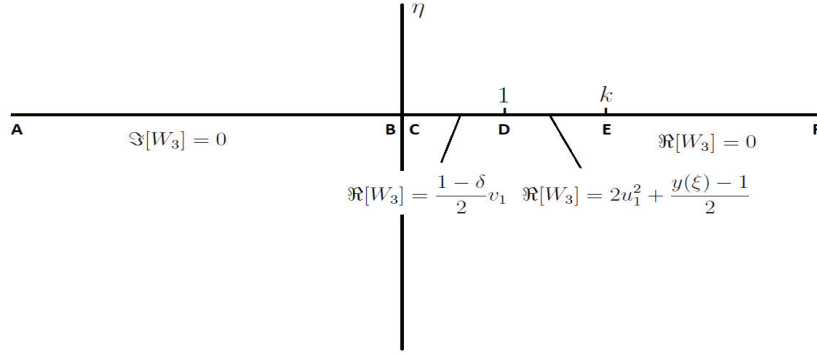
Figure 5.5. Second order problem with the unknown function W_3

Then we guarantee the behaviour of the multiplication function $W_4(\zeta) = W_3(\zeta)\tilde{R}(\zeta)$ as $\zeta \to \infty$ is a complex constant $C_{\tilde{R}}$, which have to be determined later. We will need the constant $C_{\tilde{R}}$ to get a new function $W_5(\zeta) = W_4(\zeta) - C_{\tilde{R}}$ such that $W_5 \to 0$ as $\zeta \to \infty$. The square roots in $\tilde{R}$ are considered in each interval as we done for (4.3). Then we see that $\Re[W_4]$ can be represented by regular functions on the boundary of the lower-half plane such that

$$\Re[W_4(\xi - i0)] = \frac{1-\delta}{2\pi}\sqrt{(1-\xi)(k-\xi)}\int_1^k \left(\frac{\tau-1}{(k-\tau)\tau}\right)^{1/2}\frac{d\tau}{\tau-\xi},$$

on the interval $0 < \xi < 1$,

$$\Re[W_4(\xi - i0)] = \frac{2}{\pi^2}\sqrt{\xi(k-\xi)}\left(P.v.\int_1^k \left(\frac{\tau-1}{(k-\tau)\tau}\right)^{1/2}\frac{d\tau}{\tau-\xi}\right)^2$$
$$+ \frac{\xi-1}{2\sqrt{\xi}}\left(\delta + \frac{1}{\pi}\int_1^\xi \frac{1}{\tau}\sqrt{\frac{\tau-1}{k-\tau}}d\tau\right) - \frac{\xi-1}{2\sqrt{\xi}},$$

on the interval $1 < \xi < k$ and zero on the rest of the boundary. Let $\Re[W_4(\xi - i0)] = f_4(\xi)$ on the interval $0 < \xi < 1$ and $\Re[W_4(\xi - i0)] = g_4(\xi)$ on the interval $1 < \xi < k$. Hence the solution of this BVP-AF can be written as

$$W_4(\zeta) = \frac{i}{\pi} \left[\int_0^1 \frac{f_4(\tau)}{\tau - \zeta} d\tau + \int_1^k \frac{g_4(\tau)}{\tau - \zeta} d\tau \right]. \tag{5.6}$$

To evaluate the integral terms in (5.6), we let $I_1 = \int_0^1 \frac{f_4(\tau)}{\tau - \zeta} d\tau$ and $I_2 = \int_1^k \frac{g_4(\tau)}{\tau - \zeta} d\tau$. Then,

$$W_4(\zeta) = \frac{i}{\pi}(I_1 + I_2), \tag{5.7}$$

where

$$I_1 = \frac{1-\delta}{2\pi} \int_0^1 \left[\sqrt{(1-\tau)(k-\tau)} \int_1^k \left(\frac{s-1}{(k-s)s} \right)^{1/2} \frac{ds}{s-\tau} \right] \frac{1}{\tau - \zeta} d\tau \tag{5.8}$$

on the interval $0 < \tau < 1$ and

$$
\begin{aligned}
I_2 &= \frac{2}{\pi^2} \int_1^k \left[\sqrt{\tau(k-\tau)} \left(P.v. \int_1^k \left(\frac{s-1}{(k-s)s} \right)^{1/2} \frac{ds}{s-\tau} \right)^2 \right] \frac{1}{\tau - \zeta} d\tau \\
&+ \frac{1}{2\pi} \int_1^k \left[\frac{(\tau-1)}{\sqrt{\tau}} \int_1^\tau \frac{1}{s} \left(\frac{s-1}{k-s} \right)^{1/2} ds \right] \frac{1}{\tau - \zeta} d\tau \\
&+ \frac{\delta-1}{2} \int_1^k \frac{(\tau-1)}{\sqrt{\tau}} \frac{1}{\tau - \zeta} d\tau \\
&= I_{21} + I_{22} + I_{23}
\end{aligned}
\tag{5.9}
$$

on the interval $1 < \tau < k$. The integrals in (5.8) and (5.9) can be written by using *Sokhotski-Plemelj* formula (see Appendix D) on the boundary. For the integrals (including the *principal value* ones) in I_1, I_{21}, I_{22} and I_{23}, we rewrite them in simplified form before giving the details about calculations. Let us start with the integral in I_1 which can be calculated directly and the details of the calculations are given in Appendix A.

$$I_1 = \frac{1-\delta}{2\pi} \begin{cases} -i\pi\sqrt{(1-\xi)(k-\xi)} \int_1^k \left(\frac{s-1}{(k-s)s}\right)^{1/2} \frac{ds}{s-\xi} \\[2ex] +P.v. \int_0^1 \left(\sqrt{(1-\tau)(k-\tau)} \int_1^k \left(\frac{s-1}{(k-s)s}\right)^{1/2} \frac{ds}{s-\tau}\right) \frac{d\tau}{\tau-\xi}, \, 0 < \xi < 1, \\[2ex] \int_0^1 \left(\sqrt{(1-\tau)(k-\tau)} \int_1^k \left(\frac{s-1}{(k-s)s}\right)^{1/2} \frac{ds}{s-\tau}\right) \frac{d\tau}{\tau-\xi}, \quad \xi < 0, \quad \xi > 1. \end{cases}$$

$$I_{21} = \frac{2}{\pi^2} \begin{cases} -i\pi\sqrt{\xi(k-\xi)} \left(P.v. \int_1^k \left(\frac{s-1}{(k-s)s}\right)^{1/2} \frac{ds}{s-\xi}\right)^2 \\[2ex] +P.v. \int_1^k \sqrt{\tau(k-\tau)} \left(P.v. \int_1^k \left(\frac{s-1}{(k-s)s}\right)^{1/2} \frac{ds}{s-\tau}\right)^2 \frac{d\tau}{\tau-\xi}, \, 1 < \xi < k, \\[2ex] \int_1^k \sqrt{\tau(k-\tau)} \left(P.v. \int_1^k \left(\frac{s-1}{(k-s)s}\right)^{1/2} \frac{ds}{s-\tau}\right)^2 \frac{d\tau}{\tau-\xi}, \quad \xi < 1, \quad \xi > k. \end{cases}$$

$$I_{22} = \frac{1}{2\pi} \begin{cases} -i\pi\frac{\xi-1}{\sqrt{\xi}} \int_1^\xi \frac{1}{s}\left(\frac{s-1}{k-s}\right)^{1/2} ds \\[2ex] +P.v. \int_1^k \left(\frac{\tau-1}{\sqrt{\tau}} \int_1^\tau \frac{1}{s}\left(\frac{s-1}{k-s}\right)^{1/2} ds\right) \frac{d\tau}{\tau-\xi}, \quad 1 < \xi < k, \\[2ex] \int_1^k \left(\frac{\tau-1}{\sqrt{\tau}} \int_1^\tau \frac{1}{s}\left(\frac{s-1}{k-s}\right)^{1/2} ds\right) \frac{d\tau}{\tau-\xi}, \quad\quad \xi < 1, \quad \xi > k. \end{cases}$$

$$I_{23} = \frac{\delta-1}{2} \begin{cases} -i\pi\frac{\xi-1}{\sqrt{\xi}} + P.v. \int_1^k \frac{\tau-1}{\sqrt{\tau}} \frac{d\tau}{\tau-\xi}, \quad 1 < \xi < k, \\[2ex] \int_1^k \frac{\tau-1}{\sqrt{\tau}} \frac{d\tau}{\tau-\xi}, \quad\quad\quad \xi < 1, \quad \xi > k. \end{cases}$$

$$\int_1^k \left(\frac{s-1}{(k-s)s}\right)^{1/2} \frac{ds}{s-\xi} = \frac{2\delta}{\xi}\left(F(\frac{\pi}{2}, \sqrt{1-\delta^2}) - \Pi(\frac{\pi}{2}, \frac{(\delta^2-1)\xi}{1-\xi}\sqrt{1-\delta^2})\right), \quad (5.10)$$

where F is the complete elliptic integral of first kind and Π is the complete elliptic integral of third kind. The principal value integral in I_1 can be evaluated as

$$P.v. \int_0^1 \left(\sqrt{(1-\tau)(k-\tau)}\int_1^k \left(\frac{s-1}{(k-s)s}\right)^{1/2}\frac{ds}{s-\tau}\right)\frac{d\tau}{\tau-\xi} \quad (5.11)$$
$$= -2\delta\int_0^1 f_1(\tau)d\tau + 2\delta(k-\xi)\left[\int_0^1 \frac{f_1(\tau)-f_1(\xi)}{\tau-\xi}d\tau + f_1(\xi)\log\left(\frac{1-\xi}{\xi}\right)\right]$$

where

$$f_1(\tau) = \frac{\sqrt{1-\tau}}{\tau\sqrt{k-\tau}}\left(F(\frac{\pi}{2}, \sqrt{1-\delta^2}) - \Pi(\frac{\pi}{2}, \frac{(\delta^2-1)\xi}{1-\xi}\sqrt{1-\delta^2})\right). \quad (5.12)$$

The functions in (5.12) can be calculated numerically and the details are given in Appendix A. The first principal value integral in I_{21} can be evaluated as

$$P.v. \int_1^k \left(\frac{s-1}{(k-s)s}\right)^{1/2}\frac{ds}{s-\xi} \quad (5.13)$$
$$= 2\delta F(\frac{\pi}{2}, \sqrt{1-\delta^2}) + \frac{1-\xi}{\sqrt{\xi}}\int_1^k \frac{1}{\sqrt{s}(\sqrt{\xi}+\sqrt{s})\sqrt{(s-1)(k-s)}}. \quad (5.14)$$

The integral in (5.14) is calculated numerically and the details are given in Appendix A. The nested principal value integral in I_{21} can be evaluated as

$$P.v. \int_1^k \sqrt{\tau}(k-\tau)\left(P.v. \int_1^k \left(\frac{s-1}{(k-s)s}\right)^{1/2}\frac{ds}{s-\tau}\right)^2\frac{d\tau}{\tau-\xi} \quad (5.15)$$
$$= \frac{4}{k}F^2\left(\frac{\pi}{2}, \sqrt{\frac{k-1}{k}}\right)m_1 + m_2 + \frac{4}{\sqrt{k}}F\left(\frac{\pi}{2}, \sqrt{\frac{k-1}{k}}\right)m_3$$

where

$$m_1 = -\frac{2}{3}(k^{3/2} - 1) + (k - \xi)\left(2(\sqrt{k} - 1) - 2\sqrt{\xi}\log\frac{\sqrt{k} + \sqrt{\xi}}{1 + \sqrt{\xi}} + \sqrt{\xi}\log\frac{k - \xi}{\xi - 1}\right)$$

$$m_2 = -(\xi^2 - (2 + k)\xi + 2k + 1)\int_1^k \frac{g^2(\tau)}{\sqrt{\tau}}d\tau + (2 + k - \xi)\int_1^k g^2(\tau)\sqrt{\tau}d\tau$$
$$- \int_1^k g^2(\tau)\tau^{3/2}d\tau + (k - \xi)(1 - \xi)^2\left(\int_1^k \frac{h(\tau) - h(\xi)}{\tau - \xi}d\tau + h(\xi)\log\frac{k - \xi}{\xi - 1}\right)$$

$$m_3 = \int_1^k \tau g(\tau)d\tau + (\xi - 1 - k)\int_1^k g(\tau)d\tau + (k - \xi)(1 - \xi)\int_1^k \frac{g(\tau) - g(\xi)}{\tau - \xi}d\tau$$
$$+ (k - \xi)g(\xi)\log\frac{k - \xi}{\xi - 1}$$

and

$$g(\tau) = \int_1^k \frac{1}{\sqrt{s}(\sqrt{\tau} + \sqrt{s})\sqrt{(s - 1)(k - s)}}, \qquad h(\tau) = \frac{g^2(\tau)}{\sqrt{\tau}}.$$

The details of the above calculations are given in Appendix A. Similarly, the first integral in I_{22} can be obtained as

$$\int_1^\xi \frac{1}{s}\left(\frac{s - 1}{k - s}\right)^{1/2}ds \tag{5.16}$$
$$= 2\left[-\arctan\sqrt{\frac{k - \xi}{\xi - 1}} + \frac{1}{\sqrt{k}}\arctan\sqrt{\frac{k - \xi}{k(\xi - 1)}} + \frac{\pi(\sqrt{k} - 1)}{2\sqrt{k}}\right].$$

You can find the details in Appendix A. The principal value integral in I_{22} can be evaluated as

$$P.v. \int_1^k \left(\frac{\tau - 1}{\sqrt{\tau}}\int_1^\tau \frac{1}{s}\left(\frac{s - 1}{k - s}\right)^{1/2}ds\right)\frac{d\tau}{\tau - \xi} \tag{5.17}$$
$$= \int_1^k \frac{f(\tau)}{\sqrt{\tau}}d\tau - \frac{\xi - 1}{\sqrt{\xi}}\int_1^k \frac{f(\tau)}{\sqrt{\tau}(\sqrt{\tau} + \sqrt{\xi})}d\tau \tag{5.18}$$
$$+ \frac{\xi - 1}{\sqrt{\xi}}\left[\int_1^k \frac{f(\tau) - f(\xi)}{\tau - \xi}d\tau + f(\xi)\ln\left(\frac{k - \xi}{\xi - 1}\right)\right]$$

where the function

$$f(\tau) = \int_1^\tau \frac{1}{s}\left(\frac{s - 1}{k - s}\right)^{1/2}ds$$

satisfies the *Hölder* condition. Finally the integral and the principal value integral in I_{23} can be evaluated as

$$\int_1^k \frac{\tau - 1}{\sqrt{\tau}} \frac{d\tau}{\tau - \xi} = 2\left[\sqrt{k} - 1 + \frac{1 - \xi}{\sqrt{\xi}}\left(\arctan \frac{\sqrt{k}}{\sqrt{\xi}} - \arctan \frac{1}{\sqrt{\xi}}\right)\right] \quad (5.19)$$

$$P.v. \int_1^k \frac{\tau - 1}{\sqrt{\tau}} \frac{d\tau}{\tau - \xi} = \int_1^k \frac{1}{\sqrt{\tau}} d\tau + \frac{1 - \xi}{\sqrt{\xi}} \int_1^k \frac{d\tau}{\sqrt{\tau}(\sqrt{\tau} + \sqrt{\xi})} \quad (5.20)$$
$$+ \frac{\xi - 1}{\sqrt{\xi}} \ln \frac{k - \xi}{\xi - 1}$$

CHAPTER 6

SOLUTION BY DOMAIN DECOMPOSITION METHOD, LEADING AND SECOND ORDER

Classical dam-break problem ($H^- = 0$ for wet-bed case) is solved analytically by Korobkin and Yilmaz (Korobkin and Yilmaz, 2009). It is also solved in the master thesis of Isidici (2011) by using Eulerian variables and the Mellin transform. But there was a discontinuity problem at the point where the horizontal free surface meets the vertical free surface due to the use of Eulerian description. The Eulerian description is not suitable for the neighbourhood of the upper corner point since the liquid runs over the flow field. So it is usually difficult in such cases to use this description of a fluid motion which the area is not fixed. To use the Lagrangian description it could be better for this type of areas since the Lagrangian viewpoint of fluid mechanics focuses on each particle in the flow; it identifies each particle by its original position and this particle must be followed as time goes on. So in this chapter, we will solve the classical dam break problem at the upper corner point with Lagrangian variables at the first order and by using Domain Decomposition method at the second order. The Domain Decomposition method (DDM) is prefered because of its simplicity. We first apply the DDM to the leading order problem and compare the results of the method with those of known Fourier Series solution to determine the optimum parameters for the method. Then we apply the DDM to the second order problem with these parameters and get the second order Lagrangian solution. Hence we will get the complete solution of the free surfaces of the flow at the end of this chapter.

6.1. Classical Dam Break Problem

The classical dam-break problem investigates the initial stages of the dam break flow which is caused when a vertical dam at $x' = 0$, $-H < y' < 0$, holding the liquid at the semi infinite strip, $x' > 0$, $-H < y' < 0$, suddenly disappears. At $t' = 0$, the fluid is at rest above a rigid bed with depth H. A cartesian coordinate system (x', y') with the origin at the free surface and positive x'-axis directed along the free surface is chosen as shown in Fig. 6.1. The resulting flow is gravity driven, two dimensional and potential.

The liquid is assumed to be inviscid and incompressible.
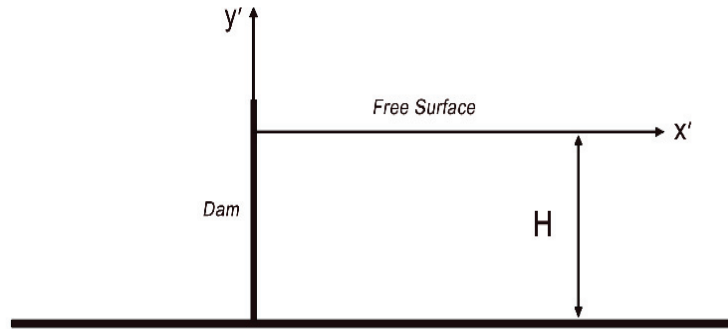
Figure 6.1. Flow region at the initial time instant $t' = 0$

Here we have two free-surfaces of the flow region, which vary in time and have to be determined as part of solution. We denote the upper horizontal part of the free-surface as $y' = \eta'(x', t')$, $x' > 0$ and the vertical part as $x' = \xi'(y', t')$. The flow region is bounded by these free-surfaces and by the rigid bottom $y' = -H$. This problem is formulated in non-dimensional variables (see Isidici (2011))

$$
\left.
\begin{aligned}
\frac{\partial u}{\partial x} + \frac{\partial v}{\partial y} &= 0 \,, \\
\frac{\partial u}{\partial t} + u\frac{\partial u}{\partial x} + v\frac{\partial v}{\partial y} &= -\frac{\partial p}{\partial x} \,, \\
\frac{\partial v}{\partial t} + u\frac{\partial v}{\partial x} + v\frac{\partial v}{\partial y} &= -\frac{\partial p}{\partial y} - 1 \,,
\end{aligned}
\right\}
\tag{6.1}
$$

$$
\text{in } -1 \le y \le \eta(x,t), \xi(y,t) \le x \le \infty
$$

$$
v = \frac{\partial \eta}{\partial t} + u\frac{\partial \eta}{\partial x} \,, \quad p = 0 \quad \text{on } y = \eta(x,t), \tag{6.2}
$$

$$
u = \frac{\partial \xi}{\partial t} + v\frac{\partial \xi}{\partial y} \,, \quad p = 0 \quad \text{on } x = \xi(y,t), \tag{6.3}
$$

$$
v(x,-1,t) = 0, \tag{6.4}
$$

$$
\eta(x,0) = \xi(y,0) = 0, \qquad u(x,y,0) = v(x,y,0) = 0, \tag{6.5}
$$

$$\text{as } x \to \infty, \, u, v \to 0 \text{ and } p \to -y, \tag{6.6}$$

where equations (6.1) are Euler equations, (6.2) and (6.3) are kinematic and dynamic boundary conditions ath the horizontal and vertical free surfaces, (6.4) is the slip boundary condition at the bottom, (6.5) is the initial conditions which states that the fluid is rest initially and (6.6) is the radiation condition at ∞, which indicates that there is no motion as $x \to \infty$.

A small-time solution to (6.1) - (6.6) may be sought by posing the power series expansions of the unknown variables, horizontal and vertical components of of velocity, horizontal and vertical free surface shapes and pressure, in time,

$$
\begin{aligned}
u &= u_0(x,y) + tu_1(x,y) + O(t^2), \\
v &= v_0(x,y) + tv_1(x,y) + O(t^2), \\
\eta &= \eta_0(x) + t\eta_1(x) + t^2\eta_2(x) + O(t^3), \\
\xi &= \xi_0(y) + t\xi_1(y) + t^2\xi_2(y) + O(t^3), \\
p &= p_0(x,y) + tp_1(x,y) + O(t^2)
\end{aligned}
\tag{6.7}
$$

as $t \to 0$, $\mathbf{x} = O(1)$, where $\mathbf{x} = (x,y)$. We find from the initial conditions that $u_0 = v_0 = 0$, $\eta_0 = \eta_1 = 0$ and $\xi_0 = \xi_1 = 0$.

By substituting the expansions (6.7) in (6.1) - (6.6) and using the Taylor series expansions of unknown functions about $y = 0$ for the vertical free surface and $x = 0$ for the horizontal free surface in the boundary conditions, we fix the domain as the semi-infinite horizontal strip, $-1 \leq y \leq 0$, $0 \leq x < \infty$ and find the following boundary value problem at the leading order as

$$\triangle p_0 = 0 \quad -1 \leq y \leq 0, 0 \leq x < \infty \tag{6.8}$$

$$p_0(x,0) = 0, \quad p_0(0,y) = 0, \quad p_{0,y}(x,-1) = -1, \quad \text{as } x \to \infty, p_0 \to -y,$$

with $u_1 = -p_{0,x}$, $v_1 = -p_{0,y} - 1$ and the series solution is

$$p_0(x,y) = -y + \sum_{n=0}^{\infty} \frac{8(-1)^n}{(2n+1)^2\pi^2} \sin\left((2n+1)\frac{\pi}{2}y\right)e^{-(2n+1)\frac{\pi}{2}x}. \tag{6.9}$$

Analysis of the singularity in $u_1 = -p_{0,x}$ near the bottom point $(0, -1)$ was studied in Isidici (2011) and the correction to the leading order was obtained. But the discontinuity at the top point (0,0) was not studied. To conduct the study and deal with the discontinuity at the top point, (0,0), we employ the Lagrangian variables. The velocities of the fluid at the leading order can be obtained by differentiating the leading order pressure (6.9),

$$u = \frac{dx}{dt} = -t \sum_{n=0}^{\infty} \frac{8(-1)^n}{(2n+1)^2 \pi^2} \left(-(2n+1)\frac{\pi}{2} \right) \sin\left((2n+1)\frac{\pi}{2} y \right) e^{-(2n+1)\frac{\pi}{2}x}, \quad t > 0,$$

(6.10)

$$v = \frac{dy}{dt} = -t \sum_{n=0}^{\infty} \frac{8(-1)^n}{(2n+1)^2 \pi^2} \left((2n+1)\frac{\pi}{2} \right) \cos\left((2n+1)\frac{\pi}{2} y \right) e^{-(2n+1)\frac{\pi}{2}x}, \quad t > 0.$$

We can find the sum of the infinite series in (6.10) as

$$\frac{dx}{dt} = -\frac{2t}{\pi} \log \sqrt{\frac{(1 - e^{-\pi x})^2 + (2\cos\frac{\pi}{2}y e^{-\pi x/2})^2}{(1 + e^{-\pi x} + 2\sin\frac{\pi}{2}y e^{-\pi x/2})^2}} \quad t > 0,$$

(6.11)

$$\frac{dy}{dt} = -\frac{2t}{\pi} \arctan\left(\frac{2\cos\frac{\pi}{2}y e^{-\pi x/2}}{1 - e^{-\pi x}} \right) \quad t > 0.$$

The solution to the coupled nonlinear differential equations (6.11) can be carried out by some numerical routine with an initial condition imposed at $t = 0$. We use adaptive step-size Runge Kutta numerical routine for the solution of the system (6.11). The shape of the free surfaces near the upper corner point $(0, 0)$ is seen in Fig. 6.2, with dotted lines denoting the initial shape at $t = 0$.

In order to derive the higher-order Lagrangian solution, we study the second order solution of the boundary problem by domain decomposition method. But to get the correct parameters for this method; the domain decomposition solution of the leading order problem is needed.

6.2. Domain Decomposition of the Problem

In this method, the domain is divided into a number of overlapping subdomains where the problem solved with unknown coefficients, and then the solutions are matched at the boundaries of the sub domains to find the unknown coefficients. We first solve the
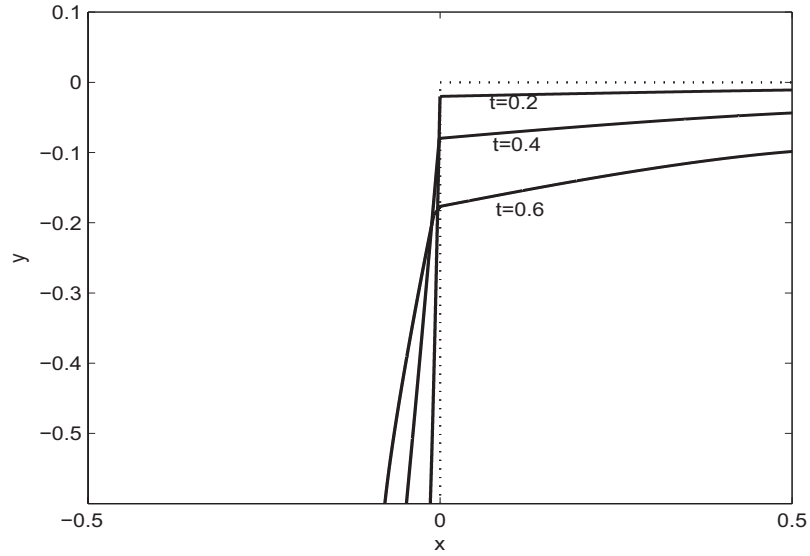
Figure 6.2. The shapes of the free surfaces in dimensionless variables at the leading
order with Lagrangian variables for $t = 0.2$, $t = 0.4$, $t = 0.6$

leading order problem by dividing the domain of the solution in three different regions
as seen in Fig. 6.3; Region 1: about the upper corner point, Region 2: about the bottom
corner point and Region 3: the domain on the right $x > 0$ as seen in Fig. 6.3.

Let r and θ represents the classical polar coordinates and $\tilde{r}$ and $\tilde{\theta}$ are the polar
coordinates for the shifted coordinates $\tilde{x} = x$ and $\tilde{y} = y + 1$. The solution in Region 1 is
written in the form:

$$p_0 = \sum_{n=1}^{\infty} C_n^I r^{2n} \sin(2n\theta), \quad -\frac{\pi}{2} \leq \theta \leq 0. \tag{6.12}$$

In Region 2,

$$
\begin{aligned}
p_0 &= -\tilde{y} + \frac{2}{\pi}\left[(1 - \log(\frac{\pi}{4}))\tilde{x} - \tilde{x}\log\tilde{r} + \tilde{\theta}\tilde{y}\right] \\
&\quad + \sum_{n=1}^{\infty} C_n^{II}\tilde{r}^{2n-1}\cos((2n-1)\tilde{\theta}), \quad 0 \leq \tilde{\theta} \leq \frac{\pi}{2}.
\end{aligned}
\tag{6.13}
$$

Figure 6.3. Sketch of the decomposition adopted

In Region 3,

$$p_0 = (1 - \tilde{y}) + \sum_{n=1}^{\infty} C_n^{III} r^{2n} \cos(\lambda_n \tilde{y}) \exp(-\lambda_n \tilde{x}), \quad \tilde{x} > 0. \qquad (6.14)$$

The idea is to find a solution of the boundary problem (6.8) by using different representations of the solutions in these three regions. The coefficients of the expansions are derived by a collocation method on a certai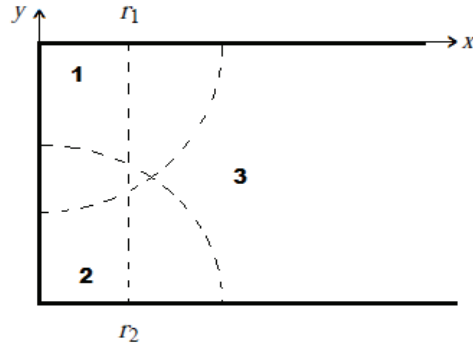n number of points. The collocation points are distributed along the lines which seperate the different domains and the matching between the representations used in the two adjacent regions is enforced. However, it is rather difficult to achieve an exact matching by using a finite series. An important limit is related to the round of errors which can be accumulated when operating with large power series. In order to circumvent the difficulty, the matching is enforced on number of points which is larger than the number of unknown coefficients. The resulting overdetermined linear system is solved in the least square fashion.

The decomposition is done by using same radius for Region 1 and Region 2 so that there is overlapping with the boundaries of the regions, $i.e.$ $r_1 = r_2$ is not smaller than half of the height of the dam. The boundary of the Region 3 is chosen as a vertical line passes at $x_3 = -r_1/2$. The coefficients of the expansions are derived by a collocation method on a certain number of points; which are chosen two times larger than the number of the unknown coefficients. The *Singular Value Decomposition* method is used to solve the overdetermined system of equations. Let N_i denotes the number of terms of the expansion

considered for region R_i and N_c the number of collocation points per each term in the expansion. Hence, $N_c N_i$ are the total number of collocation points, $i = 1, 2, 3$. Due to the peculiarity of the solution in Region 2, the number of terms for this region is chosen two times larger than the other regions. So, there are three parameters to be selected: the number of terms in the expansions N_i, the number of collocation point per term N_c and the radius r_1. We matche the solutions by using suitable parameters and then derive the corresponding coefficients of the expansion in each region. We get the best solution for the leading order using the parameters $N_1 = N_3 = 8$, $N_2 = 16$, $N_c = 8$ and $r_1 = 0.8$. In order to validate the procedure, the domain decomposition solution is compared with the analytical solution (Tables~6.1 and 6.2).

In Table 6.1 the pressure values at the line segment $x = 0.4, -0.98 < y < -0.1$ for $t = 1$ are compared and it is found that the maximum relative error is 2.036×10^{-6}. In Table 6.2, the coefficients in the expansions (6.12)-(6.13) are computed by keeping 8 terms in the expansions, which are the first numbers in the first line of columns 2, 3 and 4, but using different numbers for collocation points per term (8, 10 and 12), which are the second numbers in the first line of the columns 2, 3 and 4, are compared showing that they do not change greatly with the number of collocation points.

Table 6.1. Comparison of the leading order pressure with the analytical solution (A.S.) & domain decomposition solution (D.D.S.) at $x = 0.4$ for $t = 1$.

$x = r/2 = 0.4$	A.S.	D.D.S.	Rel. Err.
$y = -0.1$	0.03772292	0.03772284	2.036×10^{-6}
$y = -0.2$	0.07618666	0.07618652	1.838×10^{-6}
$y = -0.3$	0.11619080	0.11619080	2.012×10^{-8}
$y = -0.4$	0.15865982	0.15866034	3.285×10^{-7}
$y = -0.5$	0.2047235	0.20472455	5.050×10^{-8}
$y = -0.6$	0.25581418	0.25581716	1.167×10^{-7}
$y = -0.7$	0.31376662	0.31376923	8.324×10^{-8}
$y = -0.8$	0.38085756	0.38085983	5.978×10^{-8}
$y = -0.9$	0.45962375	0.45962585	4.558×10^{-8}
$y = -0.92$	0.47698906	0.47698698	4.348×10^{-8}
$y = -0.94$	0.49492189	0.49492395	4.160×10^{-8}
$y = -0.96$	0.51343904	0.51344109	3.988×10^{-8}
$y = -0.98$	0.53254616	0.53254820	3.832×10^{-8}

After this validation the domain decomposition method now can be applied to the second order problem. The second order problem is defined by the boundary value

problem,

$$\triangle p_2 = -2(u_{1,x}^2 + u_{1,y}^2) \quad -1 \leq y \leq 0, 0 \leq x < \infty \qquad (6.15)$$

$$p_2(x,0) = 2\eta_2^2(x) + \eta_2(x), \quad p_2(0,y) = 2\xi_2^2(y),$$

$$p_{2,y}(x,-1) = 0, \quad p_2 \to 0 \text{ as } x \to \infty.$$

The solution in Region 1, $-\frac{\pi}{2} \leq \theta \leq 0$, is written in the form:

$$p_2 = \frac{1}{2}v_1 + (v_1^2 - u_1^2)(\frac{4}{\pi}\theta + \frac{1}{2}) + \frac{8}{\pi}u_1 \log(r)(v_1 + 1) \qquad (6.16)$$

$$+\frac{8}{\pi}\theta v_1 + \frac{4}{\pi}\theta + \sum_{n=1}^{\infty} C_n^I r^{2n} \sin(2n\theta) - u_1^2.$$

In Region 2, $0 \leq \tilde{\theta} \leq \frac{\pi}{2}$

$$p_2 = \frac{3}{2}(u_1^2 - v_1^2 + 1) + \sum_{n=1}^{\infty} C_n^{II} \tilde{r}^{2n-1} \cos((2n-1)\tilde{\theta}) - u_1^2. \qquad (6.17)$$

In Region 3, $\tilde{x} > 0$

$$p_2 = \frac{1}{2}(v_1 + v_1^2 - u_1^2 + u_1)x + v_1 y + \sum_{n=1}^{\infty} C_n^{III} r^{2n} \cos(\lambda_n \tilde{y}) \exp(-\lambda_n \tilde{x}) - u_1^2. \quad (6.18)$$

Similarly, we match the solutions by using the same parameters as the leading order problem and then derive the corresponding coefficients of the expansion in each region. Hence, the velocities of the fluid at the second order can be written by using these second order solutions of the pressure $p_2(x,y)$ as

$$u = \frac{dx}{dt} = tu_1 - \frac{1}{3}(u_1 u_{1,x} + v_1 u_{1,y} + p_{2,x}), \quad t > 0, \qquad (6.19)$$

$$v = \frac{dy}{dt} = tv_1 - \frac{1}{3}(u_1 v_{1,x} + v_1 v_{1,y} + p_{2,y}), \quad t > 0. \qquad (6.20)$$

The solution to (6.19)-(6.20) can be carried out by some numerical routine adaptive step-

size Runge-Kutta method with an initial condition imposed at $t = 0$. The comparison of the shapes of the free surfaces near the upper corner point using leading and second order solutions with Lagrangian variables is given in Fig. 6.4. It is seen that the second order solution makes a larger difference in the vertical free surface than in the horizontal free surface. In Fig. 6.5, the shapes of the free surfaces near the upper corner point is plotted using both leading and second order solutions for different times. Finally the complete picture of the shapes of he free surfaces using Lagrangian description for the upper part and Eulerian description for the bottom part at the second order can be seen in Fig. 6.6.
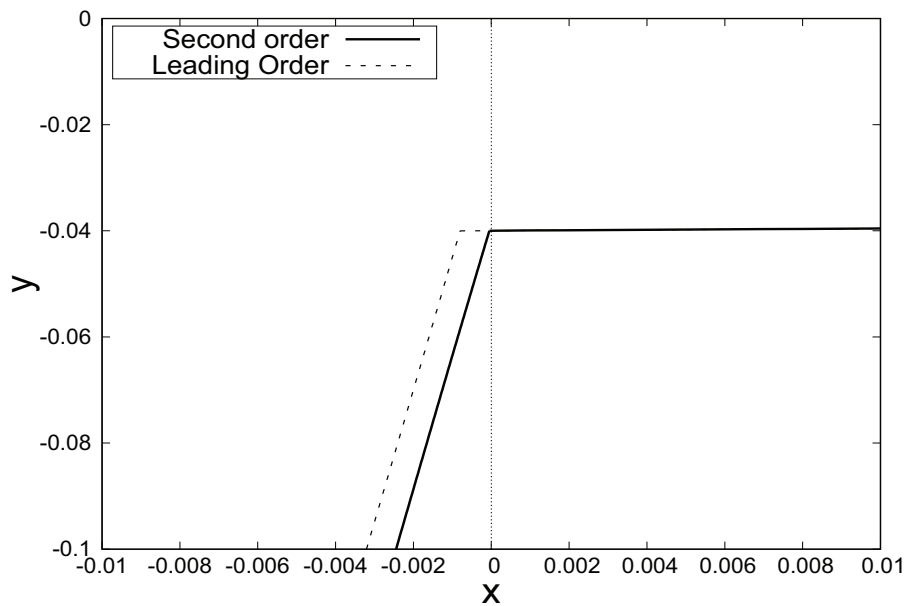

Figure 6.4. The shapes of the free surfaces in dimensionless variables with the comparison of the leading order and second order with Lagrangian variables for $t = 0.2$
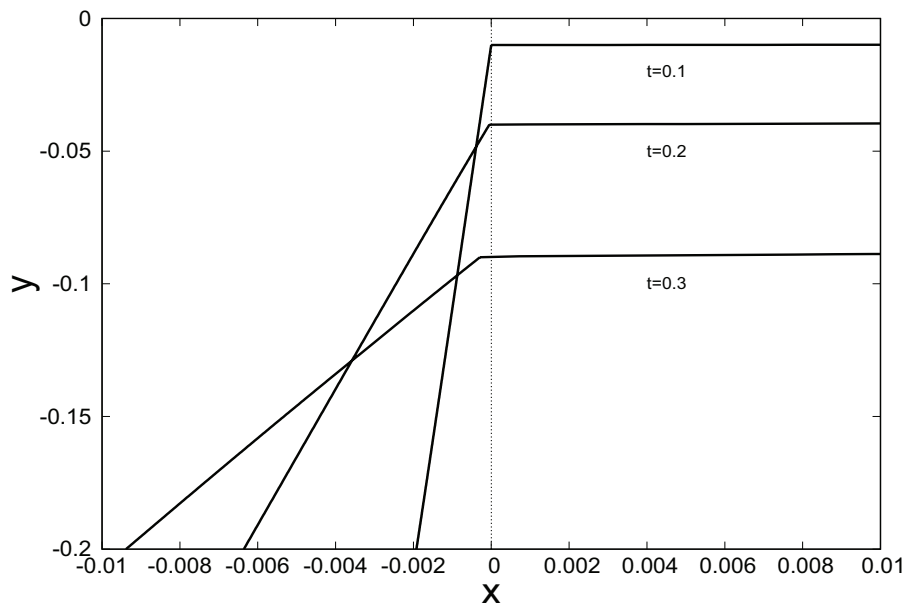
Figure 6.5. The shapes of the free surfaces in dimensionless variables at the second order with Lagrangian variables for different times
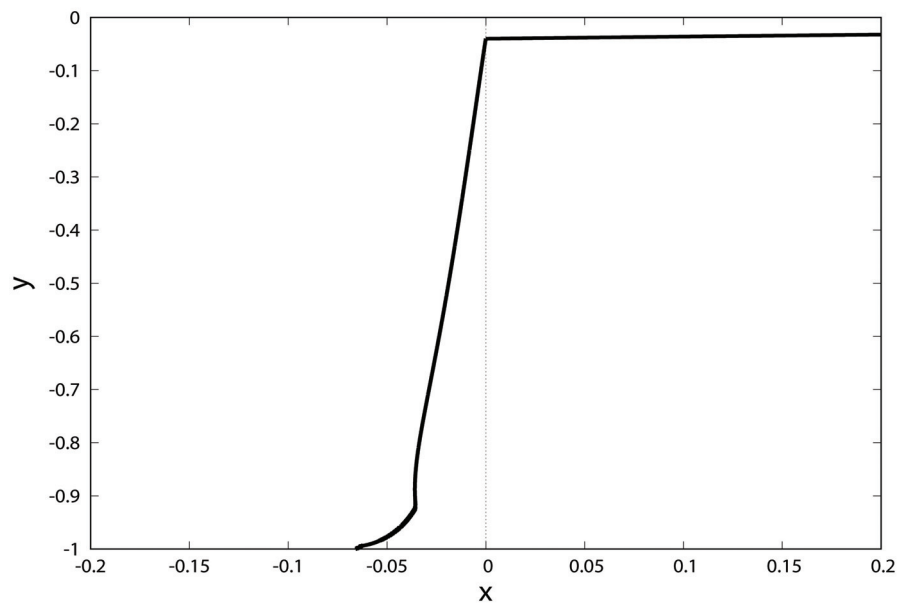

Figure 6.6. The shapes of the free surfaces at the second order for $t = 0.2$

Table 6.2. Effect of the collocation points on the coefficients

$Coef.$	8-8	8-10	8-12
C_1^A	-0.589675	-0.585556	-0.584781
C_2^A	0.161116	0.161908	0.161601
C_3^A	0.044510	0.044659	0.044744
C_4^A	0.100245	0.100737	0.101034
C_5^A	0.074988	0.075511	0.075808
C_6^A	0.136470	0.138244	0.139307
C_7^A	0.158118	0.160940	0.162633
C_8^A	0.200447	0.200983	0.201161
C_1^B	0.17168	0.170632	0.169947
C_2^B	0.152807	0.153092	0.153275
C_3^B	0.061146	0.061409	0.061579
C_4^B	0.042178	0.042119	0.042081
C_5^B	0.033989	0.034421	0.034701
C_6^B	0.049782	0.049885	0.049947
C_7^B	0.049615	0.049748	0.049828
C_8^B	0.023350	0.025080	0.026204
C_9^B	0.064207	0.064415	0.064544
C_{10}^B	0.105125	0.105555	0.105819
C_{11}^B	0.049159	0.054885	0.058603
C_{12}^B	0.148866	0.148929	0.148907
C_{13}^B	0.181092	0.184229	0.186180
C_{14}^B	-0.052022	-0.030383	-0.016215
C_{15}^B	0.508789	0.504884	0.502257
C_{16}^B	0.718653	0.732841	0.741539
C_1^C	-0.414390	-0.415800	-0.416708
C_2^C	1.525835	1.527664	1.528866
C_3^C	-1.864034	-1.865337	1.866100
C_4^C	6.345436	6.356601	6.363730
C_5^C	-13.89871	-13.92205	-13.93554
C_6^C	49.18452	49.38880	49.51692
C_7^C	-105.4966	-105.5670	-105.5876
C_8^C	425.9344	427.5115	428.4633

CHAPTER 7

CONCLUSION

In this thesis, the main interest is the dam break problem of wet-bed case during the initial times of the flow. This problem is examined in three ways; by using Fourier series method, variational method and the conformal mapping. All positive and negative aspects of these methods are discussed in this thesis. In addition, this thesis involves second order solution to dam break problem of dry-bed case as a continuation of master thesis of Isidici (2011).

In the first chapter, we begin with the mathematical formulation of the problem. Then we continue with small-time behaviour of the problem and give an explanation about the importance of the initial stages in the second chapter. The Fourier series solution is also given in this chapter with its deficiencies.

In Chapter 3, the variational method is introduced. The application of the Galerkin method to the dam break problem gives good results at the interface with an accurate choice of the test functions. But there occurs adversities on application of Galerkin method to the other part of the boundaries which reveals the necessity of a new method.

In Chapter 4, the conformal mapping idea helps to find the analytical solution of the problem for the case of equal densities in each side at the whole boundary. The derivation of the conformal mapping and its application to the problem is stated in this chapter clearly. Immediately after this chapter, Chapter 5 contains the second order analytical solution of dam break problem by using the same conformal mapping and similar complex analysis techniques.

Finally in Chapter 6, we introduce the domain decomposition method which is convenient to use in fluid flow problems. The second order solution of free-surfaces are obtained and full shape of the free-surface is drawn more explicitly.

This thesis investigates the method of Fourier series, the variational approaches and the conformal mapping technique in the solution of the dam break problem. It is concluded that the conformal mapping technique has the advantage of obtaining the solution in the whole domain boundary with accurate results. The Fourier series solution that is used in the leading order problem has convergency problems near the contact points, where some kind of singularity is expected. The variational technique, on the other hand, can be used successfully on the interface. However on the other parts of the boundary

where there is free surface, the variational technique fails.

REFERENCES

Cai, X. (2003). Overlapping domain decomposition methods. *Lecture Notes in Computational Science and Engineering*.

Chwang, A. T. (1983). Nonlinear hydrodynamic pressure on an accelerating plate. *Physics of Fluids (1958-1988)*.

Dalrymple, R. A. (1989). Water waves past abrupt channel transitions. *Applied Ocean Research*.

Dressler, R. F. (1952). Hydraulic Resistance Effect Upon the Dam-Break Functions. *Journal of Research of the National Bureau of Standards*.

Evans, D. V. and C. A. N. Morris (1972). Complementary approximations to the solution of a problem in water waves. *J. Inst. Maths. Applics.*.

Evans, D. V. and R. Porter (1995). Complementary approximations to wave scattering by vertical barriers. *Journal of Fluid Mechanics*.

Gallagher, M. (2015). *The initial development of a jet caused by fluid, body and free surface interaction*. Ph. D. thesis, University of Birmingham.

Glowinski, R., Q. V. Dinh, and J. Periaux (1983). Domain decomposition methods for nonlinear problems in fluid dynamics. *Computer Methods in Applied Mechanics and Engineering*.

Greenhow, M. (1987). Wedge entry into initially calm water. *Applied Ocean Research*.

Greenhow, M. and W. Lin (1983). Nonlinear-Free Surface Effects: Experiments and Theory. *Massachusetts Inst of Tech Cambridge Dept of Ocean Engineering*.

Isidici, D. (2011). The initial stages of gravity driven flows. Master's thesis, Izmir Institute of Technology.

J.J.Stoker (1958). *Water Waves: The Mathematical Theory with Applications*. John Wiley

Sons, Inc.

Joo, S. W., M. A. F. S. W. W. (1989). Uniformly valid solutions to the initial-value wave-maker problem. *J. Fluid ,Mech.*.

King, A.C., N. D. (1994). The initial development of a jet caused by fluid, body and free-surface interaction. Part 1. A uniformly accelerating plate. *J. Fluid Mech.*.

Korobkin, A. and O. Yilmaz (2009). The initial stage of dam-break flow. *Journal of Engineering Mathematics*.

Lin, W. M. (1984). *Nonlinear motion of the free surface near a moving body*. Ph. D. thesis, MIT, Dept. of Ocean Engineering.

Mandal, B. N. and D. P. Dolai (1994). Oblique water wave diffraction by thin vertical barriers in water of uniform finite depth. *Applied Ocean Research*.

McIver, P. (1985). Scattering of water waves by two surface-piercing vertical barriers. *IMA J. Appl. Math.*.

Miles, J. (1967). Surface-wave damping in closed basins. *Proc. R. Soc. Lond.*.

Needham, D. J., J. Billingham, and A. C. King (2007). The initial development of a jet caused by fluid, body and free-surface interaction. Part 2. An impulsively moved plate. *Journal of Fluid Mechanics*.

Needham, D. J., P. G. Chamberlain, and J. Billingham (2008). The initial development of a jet caused by fluid, body and free surface interaction. Part 3. An inclined accelerating plate. *Quarterly Journal of Mechanics and Applied Mathematics*.

Peregrine, D. H. (1983). Flow due to a vertical plate moving in a channel. *Unpublished note, University of Madison*.

Pohle, F. (1950). *The Lagrangian equations of hydrodynamics: solutions which are analytic functions of the time*. Ph. D. thesis, New York University.

Porter, R. (1995). *Complementary approximations to wave scattering by vertical barriers*.

Ph. D. thesis, University of Bristol.

Quarteroni, A. and A. Valli (1999). *Domain decomposition methods for partial differential equations (Numerical Mathematics and Scientific Computation)*. Oxford University Press.

Ritter, A. (1892). Die Fortpflanzung von Wasserwellen. *Zeitschrift Verein Deutscher Ingenieure*.

Schwinger, J. and D. Saxon (1968). *Discontinuities in Waveguides*. Gordon and Breach.

Stansby, P. K., A. Chegini, and T. C. Barnes (1998). The initial stages of dam-break flow. *Journal of Fluid Mechanics*.

Whitham, G. (1892). The effects of hydraulic resistance in the dam-break problem. *Proc. R. Soc. London*.

Yilmaz, O., A. Korobkin, and A. Iafrati (2013). The initial stage of dam-break flow of two immiscible fluids. Linear analysis of global flow. *Applied Ocean Research*.

APPENDIX A

CALCULATION OF THE INTEGRALS

▶ $\int_1^\tau \frac{1}{s} \sqrt{\frac{s-1}{k-s}} ds$,   for $1 < \tau < k$, $\xi > k$. Use basic substitution $\sqrt{\frac{k-s}{s-1}} = u$,

$$= 2(1-k) \int \frac{1}{(u^2+1)(u^2+k)} du$$

$$= 2\left[-\int \frac{1}{u^2+1} + \int \frac{1}{u^2+k} \right]$$

$$= 2\left[-\arctan u + \frac{1}{\sqrt{k}} \arctan \frac{u}{\sqrt{k}} \right]$$

$$= 2\left[-\arctan \sqrt{\frac{k-s}{s-1}} + \frac{1}{\sqrt{k}} \arctan \sqrt{\frac{k-s}{k(s-1)}} \right]_1^\tau$$

$$= 2\left[-\arctan \sqrt{\frac{\tau-k}{1-\tau}} + \frac{1}{\sqrt{k}} \arctan \sqrt{\frac{\tau-k}{k(1-\tau)}} + \frac{\pi}{2} - \frac{\pi}{2\sqrt{k}} \right].$$

▶ $\int_1^k \frac{\tau-1}{\sqrt{\tau}} \frac{d\tau}{\tau-\xi}$,   for $\xi < 1$, $\xi > k$. Use basic substitution $\sqrt{\tau} = u$,

$$= 2\int_1^{\sqrt{k}} \frac{u^2-1}{u^2-\xi} du$$

$$= 2\int_1^{\sqrt{k}} \left(1 + \frac{\xi-1}{u^2-\xi}\right) du$$

$$= 2\left[\int_1^{\sqrt{k}} 1 du + (\xi-1)\int_1^{\sqrt{k}} \frac{1}{u^2-\xi} \right]$$

$$= 2\left[\sqrt{k} - 1 + \frac{1-\xi}{\sqrt{\xi}} \left(\arctan \frac{\sqrt{k}}{\sqrt{\xi}} - \arctan \frac{1}{\sqrt{\xi}} \right) \right].$$

▶ $P.v. \int_1^k \frac{\tau-1}{\sqrt{\tau}} \frac{d\tau}{\tau-\xi}$,   for $1 < \xi < k$.

$$= \int_1^k \frac{1}{\sqrt{\tau}} d\tau + (\xi-1) P.v. \int_1^k \frac{1}{\sqrt{\tau}(\tau-\xi)} d\tau$$

$$= \int_1^k \frac{1}{\sqrt{\tau}} d\tau + (\xi-1) P.v. \int_1^k \frac{1}{\sqrt{(\tau-\xi)}} \left(\frac{1}{\sqrt{\tau}} - \frac{1}{\sqrt{\xi}} + \frac{1}{\sqrt{\xi}} \right) d\tau$$

$$= \int_1^k \frac{1}{\sqrt{\tau}} d\tau + (1-\xi) \int_1^k \frac{d\tau}{(\sqrt{\tau}+\sqrt{\xi})\sqrt{\tau}\sqrt{\xi}} + \frac{\xi-1}{\xi} P.v. \int_1^k \frac{d\tau}{\tau-\xi}$$

$$= \int_1^k \frac{1}{\sqrt{\tau}} d\tau + (1-\xi) \int_1^k \frac{d\tau}{(\sqrt{\tau}+\sqrt{\xi})\sqrt{\tau}\sqrt{\xi}} + \frac{\xi-1}{\xi} \ln \frac{k-\xi}{\xi-1}.$$

APPENDIX B

BOUNDARY VALUE PROBLEMS OF ANALYTIC FUNCTIONS

Find analytic function $W(z)$ in $y < 0$ such that $W(z) \to 0$ as $z \to \infty$ and

$$\Re[W(x - i0)] = f(x)$$

on the real axis, where the function $f(x)$ is integrable and satisfies the *Hölder* condition. The soluion of this BVP-AF is

$$W(z) = \frac{i}{\pi} \int_{-\infty}^{\infty} \frac{f(\tau)}{\tau - z} d\tau \quad (\Im(z) < 0)$$

where $W(z) = \phi(x, y) + i\psi(x, y)$.

APPENDIX C

SOKHOTSKI-PLEMELJ FORMULA

Let f be a complex-valued function which is defined and continuous on the real line, then

$$\lim_{y \to 0^-} \left(\int_{-\infty}^{\infty} \frac{f(\tau)}{\tau - z} d\tau \right) = -i\pi f(x) + P.v. \int_{-\infty}^{\infty} \frac{f(\tau)}{\tau - x} d\tau,$$

where $P.v.$ denotes the Cauchy principal value.

APPENDIX D

CAUCHY-RIEMANN EQUATIONS

Let f be a complex-valued function of a single complex variable $z = x + iy$, such that $f(x + iy) = u(x, y) + iv(x, y)$. Suppose that the real (u) and imaginary (v) parts of f are real-differentiable at a point in an open subset of $\mathbb{C}$ (the set of complex numbers). If u and v satisfies the equations,

$$\frac{\partial u}{\partial x} = \frac{\partial v}{\partial y},$$
$$\frac{\partial u}{\partial y} = -\frac{\partial v}{\partial x}$$

which are called Cauchy-Riemann equations.

APPENDIX E

JACOBI POLYNOMIALS

The Jacobi polynomials, also known as hypergeometric polynomials, denoted by $P_n^{(\alpha,\beta)}(x)$, are orthogonal with respect to the Jacobi weight function $w^{(\alpha,\beta)}(x) = (1 - x)^\alpha(1 + x)^\beta$ over $I = (-1, 1)$ with $\alpha, \beta > -1$, namely

$$\int_{-1}^{1} P_n^{(\alpha,\beta)}(x)P_m^{(\alpha,\beta)}(x)w^{(\alpha,\beta)}(x)dx = \gamma_n^{\alpha,\beta}\delta_{mn}, \qquad \text{(E.1)}$$

where $\gamma_n^{\alpha,\beta} = \|P_n^{(\alpha,\beta)}\|_{w^{(\alpha,\beta)}}^2$. They are solutions to the Jacobi differential equation,

$$(1 - x^2)y'' + [\beta - \alpha - (\alpha + \beta + 2)x]y' + n(n + \alpha + \beta + 1)y = 0 \qquad \text{(E.2)}$$

and give some other special named polynomials as special cases (For $\alpha = \beta = -\frac{1}{2}$, it is named as Chebyshev Polynomials).

The Jacobi polynomials can be written in terms of the Gamma function explicitly,

$$P_m^{(\alpha,\beta)}(x) = \frac{\Gamma(\alpha + m + 1)}{m!\Gamma(\alpha + \beta + m + 1)}\sum_{n=0}^{m} \binom{m}{n} \frac{\Gamma(\alpha + \beta + m + n + 1)}{2^n\Gamma(\alpha + n + 1)}(x - 1)^n$$

and satisfy the following three-term reccurence relation

$$\begin{aligned}
P_{m+1}^{(\alpha,\beta)}(x) &= (a_n^{(\alpha,\beta)}x - b_n^{(\alpha,\beta)})P_m^{(\alpha,\beta)}(x) - c_n^{(\alpha,\beta)}P_{m-1}^{(\alpha,\beta)}(x), \quad n \geq 1, \\
P_0^{(\alpha,\beta)}(x) &= 1, \quad P_1^{(\alpha,\beta)}(x) = \frac{1}{2}(\alpha + \beta + 2)x + \frac{1}{2}(\alpha - \beta),
\end{aligned}$$

where

$$a_n^{(\alpha,\beta)} = \frac{(2n+\alpha+\beta+1)(2n+\alpha+\beta+2)}{2(n+1)(n+\alpha+\beta+1)},$$

$$b_n^{(\alpha,\beta)} = \frac{(\beta^2-\alpha^2)(2n+\alpha+\beta+1)}{2(n+1)(n+\alpha+\beta+1)(2n+\alpha+\beta)},$$

$$c_n^{(\alpha,\beta)} = \frac{(n+\alpha)(n+\beta)(2n+\alpha+\beta+2)}{(n+1)(n+\alpha+\beta+1)(2n+\alpha+\beta)}.$$

This relation allows us to evaluate the Jacobi polynomials at any given abscissa $x \in [-1, 1]$.

VITA

Date and Place of Birth: 26.06.1986, İzmir - Turkey

EDUCATION

2012 - 2018 Doctor of Philosophy in Mathematics

Graduate School of Engineering and Sciences, İzmir Institute of Technology

Thesis: Short Time Behaviour of Dam Break Flow Involving Two Liquids

2009 - 2011 Master of Science in Mathematics

Graduate School of Engineering and Sciences, İzmir Institute of Technology

Thesis: The Initial Stages of Gravity Driven Flows

Supervisor: Prof. Dr. Oğuz YILMAZ

2006 - 2011 Bachelor of Mathematics

Department of Mathematics, Dokuz Eylül University

PROFESSIONAL EXPERIENCE

2010 - 2018 Research and Teaching Assistant

Department of Mathematics, İzmir Institute of Technology